

BEAM-PLASMA INTERACTION IN ASTRON*

C. D. STRIFFLER† and T. KAMMASH

Department of Nuclear Engineering, University of Michigan, Ann Arbor,
Mich. 48105, U.S.A.

(Received 19 June 1972; and in final form 15 January 1973)

Abstract—The beam-plasma interactions in the Astron device are examined utilizing a model which consists of a homogeneous, cold, relativistic electron beam (*E*-Layer particles) streaming through a Maxwellian plasma normal to a uniform external magnetic field. Using linear stability analysis, the model shows that the strongest interactions occur at beam harmonics in the vicinity of the plasma normal modes which are near the upper hybrid frequency, and above each subsequent multiple of the plasma electron cyclotron frequency. The possible stabilizing effects of collisions between plasma electrons and background neutral particles, as well as the energy spread for beam particles are also examined. It is shown that collisional effects are especially strong at collision frequencies of the order of the beam cyclotron frequency and that the combined effects of collisions and energy spread may lead to quenching of the unstable modes. Comparison of the analytical results with experimental observations is presented and discussed.

1. INTRODUCTION

THE INTERACTION of a beam of charged particles with a target plasma and its relevance to many areas of plasma physics has been the subject of many investigations in recent years (BRIGGS, 1964; WATSON *et al.*, 1960; SINGHAUS, 1964; KUSSE *et al.*, 1970; BOGDANKEVICH *et al.*, 1971; BÖHMER *et al.*, 1971; SELF *et al.*, 1971; KAINER *et al.*, 1972). The various roles that such a beam plays when propagating through a plasma are indeed numerous. One role that has been receiving increasing attention is that in which the beam transfers some of its streaming energy into thermal energy of the plasma, thus heating it. An even more basic role is that in which the beam is used to create a plasma via ionization of a background neutral gas.

Another role, in which the beam may be used, is to form a closed magnetic region to confine a plasma. The Astron Thermonuclear Machine is such a device (CHRISTOFILOS *et al.*, 1958, 1968). A closed system of magnetic field lines is created in the vicinity of a thin shell of circulating electrons called the *E*-Layer. These *E*-Layer particles circulate about an external magnetic axis and are confined in their axial motion by mirror fields. As the density of these *E*-Layer particles increases the self-magnetic field produced by them also increases until the combination of external and beam self-field gives rise to a closed system of field lines.

As the *E*-Layer particles enter the Astron system they interact with neutral particles. This interaction leads to ionization of the gas and subsequent creation of a plasma. Because of the space charge of the beam, the plasma electrons are initially ejected out of the region of the *E*-Layer where the ionization has occurred. The plasma ions on the other hand are attracted to the region and continue to build up in concentration. When sufficient plasma has been formed so that the space charge of the beam has been charged neutralized by the plasma ions, further ionization allows the plasma electrons to remain in the *E*-Layer region so that charge neutrality is maintained. Obviously, when a large amount of plasma has been created, the entire beam-plasma system appears to be that of a low density beam of charged particles propagating through a dense plasma, which itself is approximately charge neutral. When this stage is

* This work is supported in part by the U.S. Atomic Energy Commission.

† Present Address: Resident Research Associate at the Naval Research Laboratory, Washington, D.C. 20390, U.S.A.

arrived at in the evolution of an Astron experiment, it is followed by the appearance of radiation at certain harmonics of the beam cyclotron frequency (the orbits of the beam particles are approximately circular due to the external magnetic field). This event occurs long before sufficient beam density has been reached such that the self-magnetic field of the beam becomes any significant portion of the applied magnetic field. The observed radiation has been postulated to be due to a beam-plasma interaction, since it appears near those beam harmonics in the vicinity of the plasma upper hybrid frequency. This interaction has been labeled the "Hybrid Mode," by FESSENDEN *et al.* (1970).

The interaction between a dilute beam of charged particles and a dense plasma results from the coupling of the electric and magnetic fields of the plasma to the charged particles of the beam. In the case of the Astron system, the highly relativistic beam interacts with the electric field associated with the normal modes of the plasma resulting in energy transfer from the beam to these modes. The subsequent division of this transferred energy into field and particle kinetic energy can result in plasma heating, as discussed by LOVELACE *et al.* (1971). This article is not concerned with the ultimate disposition of this energy, but will find and attempt to understand the conditions that give rise to this transfer of energy from the beam to the plasma. It is hoped that by studying these initial events one can better delineate the direction in which a nonlinear theory is to proceed in order to discuss the final partition of energy between beam, plasma particles and field energy.

From the above description of the system of interest, a base model is proposed to study the beam-plasma interaction in Astron, and is presented in the next section. It consists of a linear stability analysis of a homogeneous, cold, relativistically streaming beam of electrons propagating through a cold, homogeneous plasma immersed in a uniform magnetic field (STIX, 1962; MONTGOMERY and TIDMAN, 1964; HOLT and HASKELL, 1965). For a cold plasma, a branch of the extraordinary normal modes occurs near the plasma upper hybrid frequency and comprises the modes for which the beam-plasma interaction can probably occur (CHRISTOFILOS, 1968; BERNSTEIN, 1958). Our model shows that the strongest interaction does occur at those beam harmonics in the vicinity of these modes.

When thermal properties of the plasma are included, unstable beam-plasma modes appear at harmonics in the region of the second and subsequent plasma electron cyclotron frequencies as well as near the upper hybrid frequency. These results are presented in Section 3 for a Cold Beam-Warm Plasma Model.

As possible mechanisms for the observed quenching of unstable modes, we consider in Sections 4 and 5, respectively, the effects of plasma electron-neutral particle collisions and energy spread in beam particles. The similarity of the resulting dispersion equation to that of the electrostatic streaming instability is noted (BRIGGS, 1964). This resemblance is noted because the two phenomena result from almost counter conditions of the wave properties, yet the interaction mechanism is exactly the same.

2. COLD BEAM-COLD PLASMA MODEL

The first model proposed to explain the beam-plasma interaction in Astron consists of a cold relativistic streaming electron beam interacting with the "extraordinary" modes of a cold plasma (STIX, 1962). The reason for examining these modes is that

the relationship between their frequency and wave number places them near the upper hybrid frequency of the plasma, where the experimental observations indicate that r.f. radiation appears. Likewise, these modes have an electric field component parallel to the direction of beam propagation, thus allowing the charged particles of the beam to interact with the electric field of the normal modes of the background plasma. The spectrum of wavelengths examined is such that a localized plane wave analysis is employed, i.e. the wavelengths of the oscillation are much smaller than any geometrical dimension of the system. With the neglect of finite boundary effects, the techniques of infinite, homogeneous theory are applicable.

We consider the response of the beam and plasma to an arbitrary electromagnetic plane wave whose electric and magnetic fields are given by

$$\begin{aligned} \mathbf{E}(\mathbf{x}, t) &= \boldsymbol{\epsilon}(\mathbf{k}, \omega)e^{i\mathbf{k}\cdot\mathbf{x}-i\omega t} \\ \mathbf{B}(\mathbf{x}, t) &= \mathbf{b}(\mathbf{k}, \omega)e^{i\mathbf{k}\cdot\mathbf{x}-i\omega t}. \end{aligned} \tag{1}$$

Response, in this case, means induced current density caused by the electromagnetic wave on the beam and plasma species. The relationship between the field vectors of the wave and the induced current density of the species is given by Maxwell's equations:

$$\begin{aligned} \nabla \times \mathbf{E} &= -\frac{1}{c} \frac{\partial \mathbf{B}}{\partial t} \\ \nabla \times \mathbf{B} &= \frac{1}{c} \frac{\partial \mathbf{E}}{\partial t} + \frac{4\pi}{c} \mathbf{J} \\ \nabla \cdot \mathbf{E} &= 4\pi\rho \\ \nabla \cdot \mathbf{B} &= 0, \end{aligned} \tag{2}$$

where \mathbf{J} and ρ are respectively the current and charge density of the medium species. Considering a cartesian coordinate system, the following wave equation is obtained,

$$\mathbf{k} \times (\mathbf{k} \times \boldsymbol{\epsilon}) + \frac{\omega^2}{c^2} \boldsymbol{\epsilon} = -\frac{4\pi i\omega}{c^2} \mathbf{J}(\boldsymbol{\epsilon}), \tag{3}$$

where the induced current density, $\mathbf{J}(\boldsymbol{\epsilon})$, for the beam-plasma system of interest is given by

$$\mathbf{J}(\boldsymbol{\epsilon}) = \mathbf{J}_{\text{BEAM}}(\boldsymbol{\epsilon}) + \mathbf{J}_{\text{PLASMA}}(\boldsymbol{\epsilon}).$$

The remaining part of the analysis involves the calculation of the induced current density, with the resulting dispersion relation obtained by setting the determinant of the coefficients of the electric field components in the wave equation equal to zero.

Figure 1 shows an idealized cross-section of the Astron system pertinent to the beam-plasma interaction (CHRISTOFILOS *et al.*, 1958, 1968). It is a sector of a circular region that appears midway and perpendicular to the external magnetic field. The *E*-Layer particles rotate about the magnetic axis in approximately circular orbits of average radius R in a cylindrical shell of thickness t_{EL} .

The experimental results on the "hybrid" instability indicate that it does not appear until charge neutralization of the beam occurs (FESSENDEN *et al.*, 1970). Thus, we

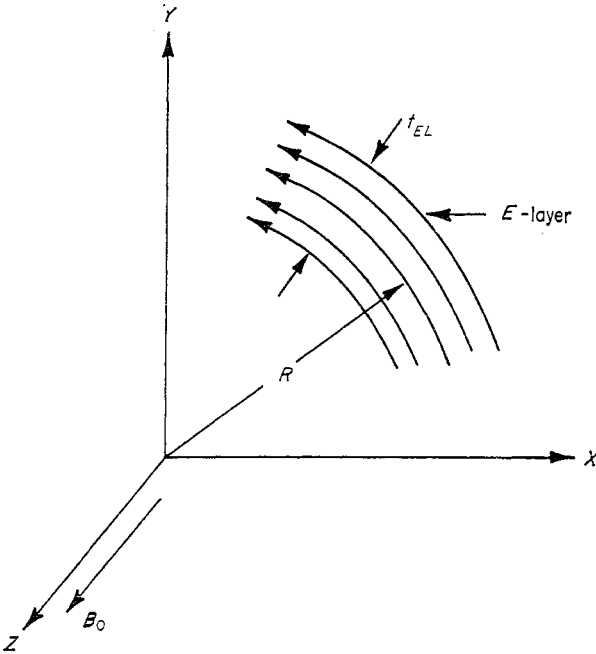


FIG. 1.—Cross-section of Astron system showing *E*-layer.

consider the following simple model of the plasma species. We assume an infinite homogeneous, cold plasma of uniform density, n_P , immersed in a constant magnetic field, \mathbf{B}_0 . Collisions between plasma particles and other particles are ignored, and the relevant equations to describe the plasma species are the fluid equations:

$$\begin{aligned} \frac{\partial n_\alpha}{\partial t}(\mathbf{x}, t) + \nabla \cdot n_\alpha \mathbf{v}_\alpha(\mathbf{x}, t) &= 0 \\ m_\alpha \frac{d\mathbf{v}_\alpha}{dt} &= q_\alpha \left[\mathbf{E}(\mathbf{x}, t) + \frac{1}{c} \mathbf{v}_\alpha \times \mathbf{B}(\mathbf{x}, t) \right] \\ \mathbf{J}_\alpha &= n_\alpha q_\alpha \mathbf{v}_\alpha, \quad \frac{d}{dt} = \frac{\partial}{\partial t} + \mathbf{v}_\alpha \cdot \nabla, \end{aligned} \quad (4)$$

where $n_\alpha(\mathbf{x}, t)$, $\mathbf{v}_\alpha(\mathbf{x}, t)$ are the density and velocity of particles of species α , whose mass is m_α and charge is q_α . Since the high frequency spectrum is under consideration, the ion motion will be ignored and only the plasma electrons will be considered to play a role in the beam-plasma interaction.

Since the *E*-Layer mean radius is approximately 40 cm, we consider the interaction to occur in a sector of the *E*-Layer where the beam particles have essentially straight line orbits. The effect of the external magnetic field on the orbits of the beam particles is therefore ignored, although the periodicity that it gives rise to in the direction of propagation of the beam is maintained. Thus, the problem reduces to that of an infinite, monoenergetic, homogeneous electron beam of density n_B , streaming at a relativistic velocity \mathbf{V}_B . Neglecting self-fields and collisions, the relevant equations

describing the beam species and its interaction with an electromagnetic wave are simply the relativistic fluid equations:

$$\begin{aligned} \frac{\partial n}{\partial t}(\mathbf{x}, t) + \nabla \cdot n\mathbf{v}(\mathbf{x}, t) &= 0 \\ \frac{d}{dt} m\mathbf{v} &= q \left[\mathbf{E}(\mathbf{x}, t) + \frac{1}{c} \mathbf{v} \times \mathbf{B}(\mathbf{x}, t) \right] \\ \mathbf{J} &= nq\mathbf{v}, \quad \frac{d}{dt} = \frac{\partial}{\partial t} + \mathbf{v} \cdot \nabla, \end{aligned} \tag{5}$$

where $n(\mathbf{x}, t)$, $\mathbf{v}(\mathbf{x}, t)$, m , q represent the density, velocity, mass and charge of the beam species respectively. Because of relativistic effects, the mass in the Lorentz equation is given by

$$m = m_0 \left(1 - \frac{\mathbf{v} \cdot \mathbf{v}}{c^2} \right)^{-1/2} = m_0 \gamma, \tag{6}$$

where γ is the relativistic mass ratio and m_0 is the rest mass of the electrons.

The linear response of the beam and plasma is obtained via normal linearization techniques, where the electromagnetic wave is assumed to perturb the system only slightly from an equilibrium state. The perturbed current density of the plasma electrons is computed by linearizing the fluid equations about the plasma equilibrium state, with its value given by

$$\frac{4\pi i\omega}{c^2} \mathbf{J}_{1P} = - \frac{\omega_{PP}^2}{c^2} \frac{\omega^2 \boldsymbol{\epsilon} - i\omega \boldsymbol{\omega}_{CP} \times \boldsymbol{\epsilon} - (\boldsymbol{\omega}_{CP} \cdot \boldsymbol{\epsilon}) \boldsymbol{\omega}_{CP}}{\omega^2 - \omega_{CP}^2}. \tag{7}$$

In this equation, the following definitions have been made:

$$\omega_{PP} = \left(\frac{4\pi q_P^2 n_P}{m_0} \right)^{1/2}$$

and

$$\omega_{CP} = |\boldsymbol{\omega}_{CP}| = \frac{q_P B_0}{m_0 c}$$

are the plasma electron and cyclotron frequencies, respectively.

Likewise, for the beam, we linearize the relativistic fluid equations about the equilibrium state and obtain for the perturbed current density of the beam particles,

$$\begin{aligned} \frac{4\pi i\omega}{c^2} \mathbf{J}_{1B} &= - \frac{\omega_{PB}^2}{c^2 (\omega - \mathbf{k} \cdot \mathbf{V}_B)^2} \left\{ (\omega - \mathbf{k} \cdot \mathbf{V}_B) \left[\omega \boldsymbol{\epsilon} + \mathbf{V}_B \times (\mathbf{k} \times \boldsymbol{\epsilon}) - \omega \frac{(\mathbf{V}_B \cdot \boldsymbol{\epsilon})}{c^2} \mathbf{V}_B \right] \right. \\ &\quad \left. + \mathbf{V}_B \mathbf{k} \cdot \left[\omega \boldsymbol{\epsilon} + \mathbf{V}_B \times (\mathbf{k} \times \boldsymbol{\epsilon}) - \omega \frac{(\mathbf{V}_B \cdot \boldsymbol{\epsilon})}{c^2} \mathbf{V}_B \right] \right\}, \end{aligned} \tag{8}$$

where

$$\omega_{PB} = \left(\frac{4\pi q_B^2 n_B}{m_0 \gamma_B} \right)^{1/2}$$

is the beam plasma frequency and $\gamma_B = (1 - V_B^2/c^2)^{-1/2}$.

Combining the perturbed current densities for the plasma and beam species, one obtains the following wave equation;

$$\begin{aligned} \mathbf{k} \times (\mathbf{k} \times \boldsymbol{\epsilon}) + \frac{\omega^2}{c^2} \boldsymbol{\epsilon} &= \frac{\omega_{PP}^2}{c^2} \frac{\omega^2 \boldsymbol{\epsilon} - i\omega \boldsymbol{\omega}_{CP} \times \boldsymbol{\epsilon} - (\boldsymbol{\omega}_{CP} \cdot \boldsymbol{\epsilon}) \boldsymbol{\omega}_{CP}}{\omega^2 - \omega_{CP}^2} + \frac{\omega_{PB}^2}{c^2 (\omega - \mathbf{k} \cdot \mathbf{V}_B)^2} \\ &\times \left\{ (\omega - \mathbf{k} \cdot \mathbf{V}_B) \left[\omega \boldsymbol{\epsilon} + \mathbf{V}_B \times (\mathbf{k} \times \boldsymbol{\epsilon}) - \omega \frac{(\mathbf{V}_B \cdot \boldsymbol{\epsilon})}{c^2} \mathbf{V}_B \right] \right. \\ &\left. + \mathbf{V}_B \mathbf{k} \cdot \left[\omega \boldsymbol{\epsilon} + \mathbf{V}_B \times (\mathbf{k} \times \boldsymbol{\epsilon}) - \omega \frac{(\mathbf{V}_B \cdot \boldsymbol{\epsilon})}{c^2} \mathbf{V}_B \right] \right\}. \quad (9) \end{aligned}$$

The geometry chosen to simulate the beam-plasma interaction of Astron is shown in Fig. 2. We examine oscillations that propagate in a plane perpendicular to the magnetic field and have wave vectors parallel and perpendicular to the beam direction. With this geometry we have

$$\begin{aligned} \mathbf{k} &= (k_x, k_y, 0) \\ \boldsymbol{\epsilon} &= (\epsilon_x, \epsilon_y, \epsilon_z) \\ \mathbf{V}_B &= (0, V_B, 0), \end{aligned} \quad (10)$$

and the x , y , z components of the wave equation can be written as,

$$\begin{aligned} k_y(k_x \epsilon_y - k_y \epsilon_x) + \frac{\omega^2}{c^2} \epsilon_z &= \frac{\omega_{PP}^2}{c^2} \frac{\omega^2 \epsilon_x + i\omega \omega_{CP} \epsilon_y}{\omega^2 - \omega_{CP}^2} + \frac{\omega_{PB}^2}{c^2} \frac{(\omega - k_y V_B) \epsilon_x + k_x V_B \epsilon_y}{\omega - k_y V_B}, \\ -k_x(k_x \epsilon_y - k_y \epsilon_x) + \frac{\omega^2}{c^2} \epsilon_y &= \frac{\omega_{PP}^2}{c^2} \frac{\omega^2 \epsilon_y - i\omega \omega_{CP} \epsilon_x}{\omega^2 - \omega_{CP}^2} + \frac{\omega_{PB}^2}{c^2} \frac{k_x V_B (\omega - k_y V_B) \epsilon_x + (\omega^2 / \gamma_B^2 + k_x^2 V_B^2) \epsilon_y}{(\omega - k_y V_B)^2}, \\ -k_x^2 \epsilon_z + \frac{\omega^2}{c^2} \epsilon_z &= \frac{\omega_{PP}^2}{c^2} \epsilon_z + \frac{\omega_{PB}^2}{c^2} \epsilon_z, \quad k_\perp^2 = k_x^2 + k_y^2. \quad (11) \end{aligned}$$

A non-trivial solution to the wave equation occurs when

$$\epsilon_x = \epsilon_y = 0; \quad \epsilon_z \neq 0,$$

which leads to the dispersion equation:

$$\omega^2 = k_\perp^2 c^2 + \omega_{PP}^2 + \omega_{PB}^2.$$

This represents a purely electromagnetic wave, which for a dilute beam, $n_B \ll n_P$, is the "ordinary" normal mode of the plasma species (STIX, 1962) and is seen to be stable.

The other non-trivial solution to the wave equation occurs when the electric field of the oscillation has the components

$$\epsilon_x, \epsilon_y \neq 0; \quad \epsilon_z = 0, \quad (12)$$

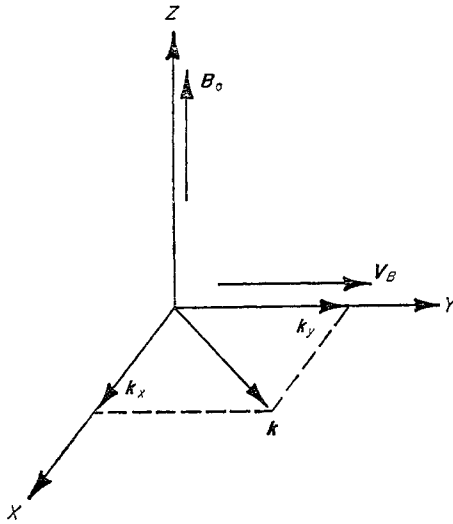


FIG. 2.—Geometry of model.

and the corresponding dispersion relation

$$\begin{aligned}
 & \left[-k_y^2 c^2 + \omega^2 - \frac{\omega^2 \omega_{PP}^2}{\omega^2 - \omega_{CP}^2} - \omega_{PB}^2 \right] \\
 & \quad \times \left[-k_x^2 c^2 + \omega^2 - \frac{\omega^2 \omega_{PP}^2}{\omega^2 - \omega_{CP}^2} - \omega_{PB}^2 \frac{\omega^2 / \gamma_B^2 + k_x^2 V_B^2}{(\omega - k_y V_B)^2} \right] \\
 & \quad - \left[k_x k_y c^2 + i \frac{\omega \omega_{CP} \omega_{PP}^2}{\omega^2 - \omega_{CP}^2} - \frac{\omega_{PB}^2 k_x V_B}{\omega - k_y V_B} \right] \\
 & \quad \times \left[k_x k_y c^2 - i \frac{\omega \omega_{CP} \omega_{PP}^2}{\omega^2 - \omega_{CP}^2} - \frac{\omega_{PB}^2 k_x V_B}{\omega - k_y V_B} \right] = 0. \tag{13}
 \end{aligned}$$

For a weak beam, the field vectors are essentially those of the extraordinary normal modes of a cold plasma. We note also, that the charged particles of the beam can interact directly with the electric field of these modes, since $\epsilon \cdot \nabla_B \neq 0$.

Before solving the beam-plasma dispersion relation, let us consider the dispersion equation in the absence of the beam. With the beam density set equal to zero, we obtain the dispersion equation for the extraordinary modes of a cold plasma, i.e.

$$(k_{\perp} c)^2 = \frac{\omega_k^2 (\omega_k^2 - \omega_{CP}^2 - 2\omega_{PP}^2) + \omega_{PP}^4}{\omega_k^2 - \omega_{CP}^2 - \omega_{PP}^2}. \tag{14}$$

A plot of this equation is shown in Fig. 3, which shows that there are two branches to these modes. One branch is below the upper hybrid frequency, $\omega_H = (\omega_{CP}^2 + \omega_{PP}^2)^{1/2}$, and the other is above. The one above is also above the velocity of light line, implying that the phase velocity of the wave is greater than the speed of light and thus no interaction with particles can occur.

From Fig. 3, the particles of the beam are expected to interact with the lower

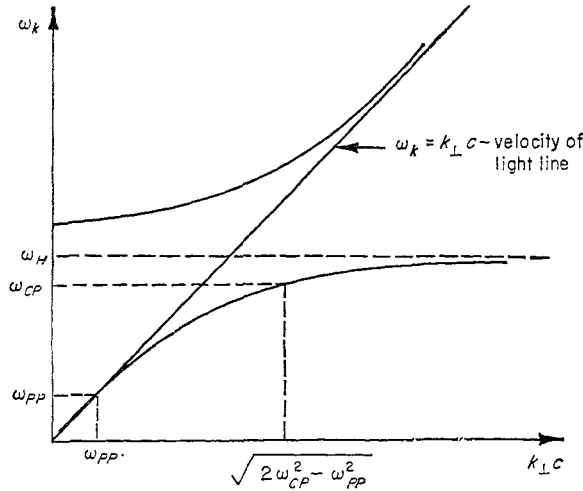


FIG. 3.—Extraordinary normal modes of a cold plasma.

branch of the normal modes between approximately the plasma frequency and the upper hybrid frequency. More explicitly, we expect the unstable solutions to the dispersion equation to have a frequency

$$\omega \sim k_y V_B \sim \omega_k, \tag{15}$$

that is, near resonance between the beam and plasma wave. Recalling the periodicity assumption in the beam model, we consider only wavelengths in the beam direction that have a certain period. Since the *E*-Layer particles are governed by cyclotron motion, such that, $\omega_{CB} = V_B/R$ is their cyclotron frequency, then the periodicity of the system becomes $2\pi R$, of which we can write,

$$k_y V_B = \frac{2\pi}{\lambda_y} R \omega_{CB} \equiv l \omega_{CB}, \tag{16}$$

where *l* is an integer and represents the periodicity of the wavelength in the beam direction. The condition implied by equation (15) is that interaction between the beam and plasma is expected at those beam cyclotron harmonics in the region of the lower branch of the plasma normal modes.

The dispersion equation given in equation (13) is solved numerically in a later section. Presently solutions are analytically examined in the region of interest with applicability to the Astron system in order to gain some insight into the major trends of the unstable modes.

Since a localized plane wave analysis has been assumed, let us consider the wavelength of the oscillation perpendicular to the beam direction, that is, λ_x , and assume a smallest dimension appropriate to Astron in that direction. Taking this dimension to be the *E*-Layer thickness, t_{EL} , one assumes for validity of the present analysis

$$\lambda_x \ll t_{EL},$$

so that boundary effects can be ignored. Specifically, we calculate a minimum value of the dimensionless parameter, $k_x c / \omega_{CB}$, which is assumed to occur when $\lambda_x = t_{EL}$.

Employing the appropriate Astron parameters, $t_{EL} = 20$ cm, $\omega_{CB} = 2\pi \times 10^8$ cps, we obtain

$$\frac{k_x c}{\omega_{CB}} \gg \left(\frac{k_x c}{\omega_{CB}/\min} \right) \equiv \frac{2\pi c}{t_{EL}\omega_{CB}} \sim 15 \tag{17}$$

as the condition that must be applied to the present model so that the Astron system can be treated by a plane wave analysis. Recalling $k_y V_B$ of equation (16) and assuming a highly relativistic beam, $V_B \sim c$, one obtains for the total perpendicular wave vector, k_{\perp} , the condition

$$\frac{k_{\perp} c}{\omega_{CB}} = \left(\frac{k_x^2 c^2}{\omega_{CB}^2} + \frac{k_y^2 c^2}{\omega_{CB}^2} \right)^{1/2} \cong \left(\frac{k_x^2 c^2}{\omega_{CB}^2} + l^2 \right)^{1/2} \cong \frac{k_x c}{\omega_{CB}} \gg 1. \tag{18}$$

When comparing this condition to Fig. 3, we see that the normal mode of interest, in this large $k_x c$ region, has a frequency very close to the upper hybrid frequency.

We now return to the cold beam-cold plasma dispersion equation, equation (13), and take the limit of large $k_x c$, and find the resulting equation to be

$$(\omega^2 - \omega_H^2)(\omega - k_y V_B)^2 - \frac{\omega_{PB}^2}{\gamma_B^2} (\omega^2 - \omega_H^2 + \gamma_B^2 \omega_{PP}^2) = 0. \tag{19}$$

We expect the unstable modes to be near harmonics of the beam cyclotron frequency, that is,

$$Re \omega \sim k_y V_B = l\omega_{CB}.$$

With this assumption, the unstable modes are obtained from the following approximate dispersion equation;

$$\begin{aligned} & \left(\frac{\omega - l\omega_{CB}}{\omega_{CB}} \right)^3 + \frac{1}{2l} \left[l^2 - \gamma_B^2 \left(1 + \frac{\omega_{PP}^2}{\omega_{CP}^2} \right) - \frac{1}{\gamma_B^2} \frac{\omega_{PB}^2}{\omega_{CB}^2} \right] \left(\frac{\omega - l\omega_{CB}}{\omega_{CB}} \right)^2 \\ & - \frac{1}{\gamma_B^2} \left(\frac{\omega_{PB}}{\omega_{CB}} \right)^2 \left(\frac{\omega - l\omega_{CB}}{\omega_{CB}} \right) - \frac{1}{2l\gamma_B^2} \left(\frac{\omega_{PB}}{\omega_{CB}} \right)^2 \left[l^2 - \gamma_B^2 \left(1 + \frac{\omega_{PP}^2}{\omega_{CP}^2} \right) + \gamma_B^4 \frac{\omega_{PP}^2}{\omega_{CP}^2} \right] = 0. \end{aligned} \tag{20}$$

The solutions obtained depend on the range of certain parameters. If one considers that the system is being examined from the stand-point of a constant beam propagating through a plasma which is increasing in density, then the important parameter to vary is ω_{PP}/ω_{CP} , which is proportional to the plasma density. This is essentially what occurs in the Astron system when the hybrid mode appears. Therefore, we treat the beam parameters, ω_{PB}/ω_{CB} and γ_B , as constants, and examine the stability at each beam harmonic, l , as a function of plasma density, ω_{PP}/ω_{CP} .

Non beam-plasma resonance

For some beam harmonics there exists a plasma density such that the hybrid frequency for this density is coincident with the beam harmonic. This density is called the hybrid density for exact beam-plasma resonance at that beam harmonic. We first consider plasma densities which do not allow this resonance to occur, i.e.

$$\frac{\omega_{PP}}{\omega_{CP}} \neq \frac{\omega_{PP}^*}{\omega_{CP}} \equiv \left(\frac{l^2 - \gamma_B^2}{\gamma_B^2} \right)^{1/2} = \frac{1}{\omega_{CP}} \left(\frac{4\pi q_P^2 n_P^*}{m_0} \right)^{1/2}. \tag{21}$$

The growth rate for this region of plasma densities is given by

$$\text{Im} \frac{\omega}{\omega_{CB}} \cong \frac{1}{\gamma_B} \left(\frac{\omega_{PB}}{\omega_{CB}} \right) \left[\frac{l^2 - \gamma_B^2(1 + \omega_{PP}^2/\omega_{CP}^2) + \gamma_B^4 \omega_{PP}^2/\omega_{CP}^2}{\gamma_B^2(1 + \omega_{PP}^2/\omega_{CP}^2) - l^2} \right]^{1/2}, \quad (22)$$

if

$$\gamma_B^2 \left(1 + \frac{\omega_{PP}^2}{\omega_{CP}^2} \right) - l^2 > 0.$$

Specializing to harmonics which are less than the plasma electron cyclotron frequency, $l < \gamma_B$, we find that for these harmonics no exact resonance occurs and thus the growth rate given in equation (22) is good for all plasma densities. In this region of harmonics the onset condition for instability is given by

$$\left(\frac{\omega_{PP}}{\omega_{CP}} \right)^2 \geq \left(\frac{\omega_{PP}}{\omega_{CP}} \right)_{\text{Onset}}^2 = \frac{\gamma_B^2 - l^2}{\gamma_B^2(\gamma_B^2 - 1)}. \quad (23)$$

This critical density decreases as the harmonic nears γ_B . That is, the critical density for the $l = 1$ harmonic is greater than for $l = 2$, etc., up to the harmonic just below γ_B . Also note, that if the plasma density terms are dominant in the growth rate expression, an asymptotic value is approached, and is given by

$$\text{Im} \frac{\omega}{\omega_{CB}} \rightarrow \frac{\omega_{PB}}{\omega_{CB}} \left(\frac{\gamma_B^2 - 1}{\gamma_B^2} \right)^{1/2}. \quad (24)$$

This is the maximum growth rate for these harmonics and is dependent on beam parameters only.

When $l = \gamma_B$, the growth rate from equation (22) is the same as that obtained above for the asymptotic result. This is expected since the condition indicated in equation (22) for $l = \gamma_B$ states that the growth rate given is not accurate at low densities. More general solutions of equation (20) are required in the low density region for the $l = \gamma_B$ harmonic.

For harmonics above the plasma electron cyclotron frequency, $l > \gamma_B$, the expression for growth rate indicates stability for plasma densities below the hybrid density, $\omega_{PP} < \omega_{PP}^*$. For densities above this value, instability results, and as the plasma density terms become dominant the asymptotic result of equation (24) is recovered. The main implication of equation (22) for these harmonics is that the growth rate is larger than the asymptotic value, that is, the asymptotic value is approached from above.

Beam-plasma resonance

We turn now to the plasma density which gives rise to exact resonance between the plasma normal mode and a given beam harmonic. We let

$$\frac{\omega_{PP}}{\omega_{CP}} = \frac{\omega_{PP}^*}{\omega_{CP}} = \left(\frac{l^2 - \gamma_B^2}{\gamma_B^2} \right)^{1/2}, \quad (25)$$

which further indicates that the resonant density increases with beam harmonic. Obviously, this region is only valid for harmonics above the plasma electron cyclotron

frequency, $l > \gamma_B$, and the growth rate at this plasma density is given by

$$\text{Im} \frac{\omega}{\omega_{CB}} \cong \frac{\sqrt{3}}{2} \left[\frac{\omega_{PB}^2 l^2 - \gamma_B^2}{\omega_{CB}^2 2l} \right]^{1/3}. \tag{26}$$

We note that this growth rate increases with l , that is, the higher the harmonic, which implies the larger the plasma density, the larger is the growth rate. As we shall see in the numerical results, this growth rate is approximately the maximum value attained at a given beam harmonic. Of course, this is not too surprising since one would expect the strongest interaction when resonance occurs. The greatest interaction should occur when the electric field of the plasma mode has its maximum component in the beam direction, and hence maximum energy transfer is likely to occur at this condition.

From the above calculations for $l > \gamma_B$, one expects an onset condition to occur at a plasma density below the hybrid density. This condition is found to be

$$\left(\frac{\omega_{PP}}{\omega_{CP}} \right)_{\text{onset}}^2 \cong \frac{(l^2 - \gamma_B^2) - 3 \left[l^2(l^2 - \gamma_B^2) \frac{\omega_{PB}^2}{\omega_{CB}^2} \right]^{1/3} \left\{ 1 - \left[\frac{l^2}{(l^2 - \gamma_B^2)^2} \frac{\omega_{PB}^2}{\omega_{CB}^2} \right]^{1/3} \right\}}{\gamma_B^2} \tag{27}$$

which is the value of plasma density for zero growth rate at beam harmonics above the plasma electron cyclotron frequency.

In summarizing this section on the cold beam-cold plasma interaction at large $k_x c / \omega_{CB}$, we have seen first that unstable modes occur near harmonics of the beam cyclotron frequency, $\text{Re } \omega \sim l \omega_{CB}$. For harmonics below the plasma electron cyclotron frequency, $l < \gamma_B$, instability with growth rate given by equation (22) exists at plasma densities above a certain critical value given in equation (23), i.e. $\omega_{PP} > (\omega_{PP})_{\text{onset}}$. This growth rate increases from zero at onset to the asymptotic value given in equation (24). The $l = \gamma_B$ harmonic possesses the same features, but more general expressions are required to obtain the appropriate result. For beam harmonics above the plasma electron cyclotron frequency, $l > \gamma_B$, an instability does not exist until a certain plasma density is reached, given in equation (27). The growth rate increases rapidly from this point to a maximum near the hybrid density, equation (26), and thereafter decreases to the asymptotic value of equation (24) via the relation given in equation (22).

In order to gain some insight into the above results, let us consider a specific set of parameters relevant to Astron, e.g. the following beam parameters (FESSENDEN *et al.*, 1970);

$$\begin{aligned} \gamma_B &= 9.0 \\ \frac{\omega_{PB}}{\omega_{CB}} &= 0.3. \end{aligned}$$

Table 1 contains the threshold plasma density for instability for these beam parameters. The onset condition for beam harmonics $l \leq 8$ is given by equation (23), while that for $l \geq 10$ by equation (27). The hybrid density is obtained from equation

TABLE 1. THRESHOLD PLASMA DENSITY FOR ASTRON BEAM PARAMETERS;
 $\gamma_B = 9.0, \omega_{PB}/\omega_{CB} = 0.3$

| l | $\left(\frac{\omega_{PP}}{\omega_{CP}}\right)_{\text{onset}}$ | $\left(\frac{l^2 - \gamma_B^2}{\gamma_B^2}\right)^{1/2}$ |
|-----|---|--|
| 1 | 0.111 | |
| 2 | 0.109 | |
| 3 | 0.105 | |
| 4 | 0.100 | |
| 5 | 0.093 | |
| 6 | 0.083 | |
| 7 | 0.070 | |
| 8 | 0.051 | |
| 9 | 0.000 | |
| 10 | 0.298 | 0.484 |
| 11 | 0.516 | 0.703 |
| 12 | 0.695 | 0.882 |

(25). For the present choice of beam parameters the asymptotic growth rate approached at all beam harmonics is

$$\text{Im} \frac{\omega}{\omega_{CB}} \rightarrow \frac{\omega_{PB}}{\omega_{CB}} \frac{V_B}{c} = 0.298.$$

The growth rates in general have been numerically calculated from the dispersion equation with arbitrary $k_x c/\omega_{CB}$. Figure 4 shows these results in the large $k_x c/\omega_{CB}$ region in which the above analytical expressions are valid. In Fig. 5, the real part of the frequency of the unstable mode, $\text{Re} \omega/\omega_{CB}$, vs ω_{PP}/ω_{CP} is shown.

From Fig. 5, one observes that for $l < \gamma_B = 9.0$, the unstable mode occurs practically at the beam harmonic. In fact, as the plasma density increases, there appears to be no shift in the position of the unstable mode in the frequency spectrum. However, for harmonics above $l = 10$, the unstable mode initially appears substantially below the harmonic frequency and then shifts toward the harmonic as plasma density

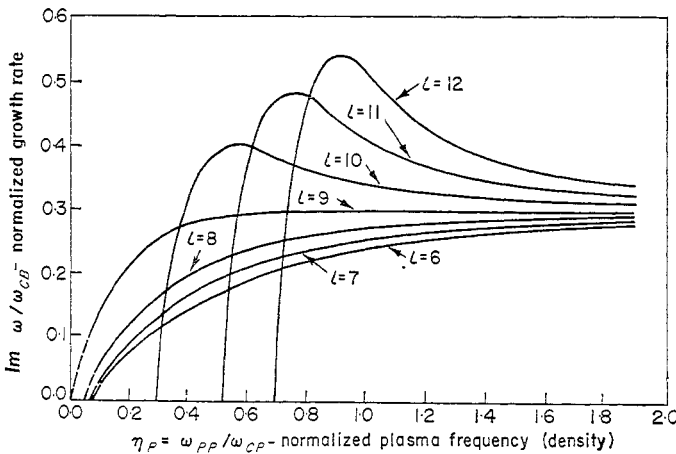


FIG. 4.—Growth rate vs plasma frequency for cold beam-cold plasma model in large $k_x c/\omega_{CB}$ region.

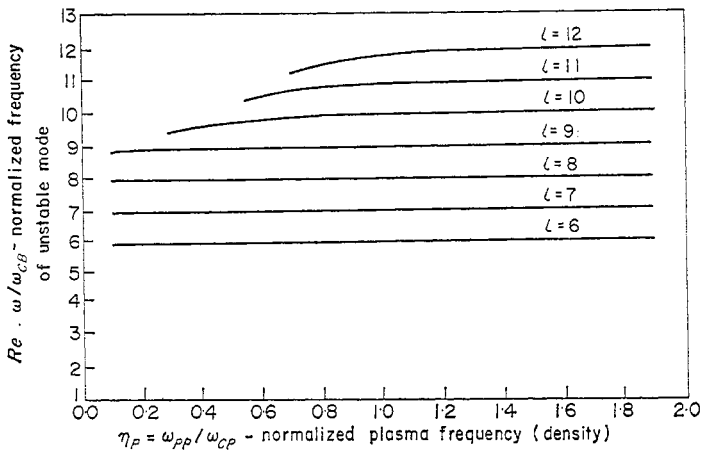


FIG. 5.—Frequency of unstable mode vs plasma frequency for cold beam-cold plasma model in large k_{zc}/ω_{CB} region.

increases. Thus, if the plasma density increased from zero to a value, such that, $\omega_{PP}/\omega_{CP} = 1.0$, the frequency band over which one would observe unstable oscillations would be larger at the higher harmonic.

The growth rate results of Fig. 4 indicate that harmonics below $\gamma_B = 9.0$ are unstable at low plasma densities. They increase monotonically from zero to the asymptotic value. Harmonics above γ_B become unstable at higher densities, though the onset density is considerably below the hybrid resonant density. The growth rate increases rapidly from onset and maximizes very close to the resonance condition between beam harmonic and plasma normal mode. Thereafter, the growth rate decreases and again approaches the asymptotic value. The higher the harmonic number, the higher the threshold density and the higher is the maximum growth rate attained. Hence, as plasma density increases, the harmonic associated with the most unstable mode also becomes larger.

The results of this cold beam-cold plasma model are very encouraging from the standpoint of comparison between theory and experiment. In one Astron experiment for which a beam energy represented by $\gamma_B \sim 8.8$, unstable modes were observed at the $l = 9, 10$ and 11 beam harmonics for the duration of the experiment (FESSENDEN *et al.*, 1970). By comparing plasma density measurements with the normalized value, ω_{PP}/ω_{CP} , our model indicates that these harmonics should be unstable. Although it predicts the "strongest" interaction to occur at those harmonics above the plasma electron cyclotron frequency, the model also indicates instabilities at beam harmonics below the plasma electron cyclotron frequency. This represents a discrepancy between theory and experiment and will be treated in a later section.

3. COLD BEAM-WARM PLASMA MODEL

In order to obtain the experimentally observed interaction at harmonics of the beam in the vicinity of the multiples of the plasma electron cyclotron frequency (FESSENDEN *et al.*, 1970) when the plasma density is low, one must take into account thermal properties of the plasma. Thermal properties give rise to normal modes of a Maxwellian plasma near integral multiples of the plasma electron cyclotron frequency.

One may also wish to ascertain the effects of very high temperatures such as would exist at thermonuclear conditions. A study of plasma temperatures ranging from 0 to 25 eV is undertaken as well as the study of the entire spectrum of wavelengths perpendicular to the beam. These results are obtained via numerical methods.

As in the previous section, we consider again the response of a beam and plasma to an arbitrary electromagnetic wave. The resulting wave equation is given in equation (3). The model of the beam species is identical to that of the previous section, where linearization of the relativistic fluid equations resulted in the perturbed current density as given in equation (8).

For the plasma species, we consider an infinite, homogeneous, Maxwellian plasma of uniform density n_P , at temperature T_P , immersed in a uniform magnetic field, \mathbf{B}_0 . Again, we ignore collisions between plasma particles as an important mechanism for the beam-plasma interaction, but include them from the standpoint of plasma temperature, so that the relevant equation for the plasma is the Vlasov equation;

$$\frac{\partial f_\alpha(\mathbf{x}, \mathbf{v}, t)}{\partial t} + \mathbf{v} \cdot \frac{\partial f_\alpha}{\partial \mathbf{x}} + \frac{q_\alpha}{m_\alpha} \left[\mathbf{E}(\mathbf{x}, t) + \frac{1}{c} \mathbf{v} \times \mathbf{B}(\mathbf{x}, t) \right] \cdot \frac{\partial f_\alpha}{\partial \mathbf{v}} = 0, \quad (28)$$

with the current density given by

$$\mathbf{J}_\alpha(\mathbf{x}, t) = q_\alpha \int d^3v v f_\alpha(\mathbf{x}, \mathbf{v}, t),$$

where $f_\alpha(\mathbf{x}, \mathbf{v}, t)$ is the distribution function of the α species. Linearization of the Vlasov equation is performed about the Maxwellian distribution

$$f_{0P}(\mathbf{v}) = n_P \left(\frac{m_0}{2\pi K T_P} \right)^{3/2} e^{-m_0 v^2 / 2K T_P}, \quad (29)$$

with K being the Boltzmann Constant, and assuming perturbations of the form $\exp(i\mathbf{k} \cdot \mathbf{x} - i\omega t)$. The resulting equations are solved for transverse waves with wave and E-vectors in the plane perpendicular to the magnetic field, \mathbf{B}_0 . The perturbed current density in component form is found to be (BERNSTEIN, 1958):

$$\begin{aligned} \frac{4\pi i \omega}{c^2} J_{1P_x} &= i \frac{\omega_{PP}^2}{c^2} \sum_{n=-\infty}^{\infty} \frac{\omega e^{-\lambda}}{\omega + n\omega_{CP}} \\ &\times \left\{ (n + i\lambda \sin 2\psi)(I_n' - I_n)\epsilon_y + i \left[\frac{n^2 I_n}{\lambda} - \lambda(1 + \cos 2\psi)(I_n' - I_n) \right] \epsilon_x \right\}, \\ \frac{4\pi i \omega}{c^2} J_{1P_y} &= - \frac{\omega_{PP}^2}{c^2} \sum_{n=-\infty}^{\infty} \frac{\omega e^{-\lambda}}{\omega + n\omega_{CP}} \\ &\times \left\{ \left[\frac{n^2 I_n}{\lambda} - \lambda(1 - \cos 2\psi)(I_n' - I_n) \right] \epsilon_y + i(n - i\lambda \sin 2\psi)(I_n' - I_n)\epsilon_x \right\}, \quad (30) \end{aligned}$$

and

$$\frac{4\pi i \omega}{c^2} J_{1P_z} = 0.$$

In addition to previous definitions and the geometry of Fig. 2, the following definitions have been made in the above equations:

$$\lambda = \frac{k_{\perp}^2 v_{TH}^2}{\omega_{CP}^2}$$

is the argument of the modified Bessel function, $I_n(\lambda)$, and its derivative I_n' ,

$$v_{TH} = \left(\frac{KT_P}{m_0}\right)^{1/2}$$

is the thermal velocity of the plasma electrons at temperature T_P , and

$$\tan \psi = \frac{k_x}{k_y},$$

where ψ is the angle between the wave vector and the y -axis.

We insert the perturbed current densities of the beam and plasma species in the wave equation for the indicated geometry and wave parameters shown in Fig. 2 with $\epsilon_z = 0$. The resulting dispersion equation for the extraordinary modes is

$$\begin{aligned} & \{\omega^2 - k_y^2 c^2 - \omega_{PB}^2 - \omega_{PP}^2 [S_1 - (1 + \cos 2\psi)S_2]\} \\ & \quad \times \{(\omega^2 - k_x^2 c^2)(\omega - k_y V_B)^2 - \omega_{PB}^2(\omega^2/\gamma_B^2 + k_x^2 V_B^2) \\ & \quad - \omega_{PP}^2(\omega - k_y V_B)^2 [S_1 - (1 - \cos 2\psi)S_2]\} \\ & \quad - \{[k_x k_y c^2 - \omega_{PP}^2 S_2 \sin 2\psi](\omega - k_y V_B) - \omega_{PB}^2 k_x V_B\}^2 \\ & \quad - \{\omega_{PP}^2(\omega - k_y V_B)S_3\}^2 = 0, \end{aligned} \tag{31}$$

where S_1 , S_2 and S_3 are summation terms given by

$$\begin{aligned} S_1 &= 2 \sum_{n=1}^{\infty} \frac{\omega^2}{\omega^2 - n^2 \omega_{CP}^2} \frac{n^2 e^{-\lambda} I_n}{\lambda}, \\ S_2 &= \lambda(e^{-\lambda} I_0)' + 2 \sum_{n=1}^{\infty} \frac{\omega^2}{\omega^2 - n^2 \omega_{CP}^2} \lambda(e^{-\lambda} I_n)', \\ S_3 &= -2 \sum_{n=1}^{\infty} \frac{n^2 \omega \omega_{CP}}{\omega^2 - n^2 \omega_{CP}^2} (e^{-\lambda} I_n)'. \end{aligned} \tag{32}$$

In the limit of a cold plasma, $v_{TH} = 0$, $\lambda = 0$, the results of the previous section are regained.

Upon examining the dispersion equation given by equation (31), we see that the equation is of infinite order in the variable ω . However, for a beam with a relativistic mass ratio of $\gamma_B = 9.0$, we find it sufficient to limit stability analysis only to beam harmonics up to $l = 20$, i.e. beam harmonics interacting at most with the warm plasma modes around the second harmonic of the plasma electron cyclotron frequency. This will yield warm plasma effects which we would also expect at subsequent multiples of the plasma electron cyclotron frequency. With this in mind, accuracy of the solutions in the vicinity of the first and second plasma electron cyclotron frequency is essential, whereas, at higher frequencies accuracy of solutions of the plasma modes is not required. Thus the infinite order equation in ω is replaced by a finite polynomial

in ω by keeping only a limited number of terms in the infinite sums. The number of terms required to obtain accurate results depends on the specific choice of system parameters. By keeping the $n = 1$ term in the sums, S_1 , S_2 and S_3 , for example, we obtain a first order effect due to thermal plasma properties on the cold hybrid mode. The $n = 1$ and 2 terms must be retained in order to obtain any plasma modes above the second plasma electron cyclotron frequency, for which there is no cold plasma limit. Numerical solutions have been obtained for the dispersion equation by progressively keeping more terms in the sums, up to and including the $n = 4$ term. The convergence of the results for any choice of system parameters studied was achieved by keeping the necessary number of terms.

TABLE 2. RANGE OF PARAMETERS

| | Parameter | Range |
|--------|---------------------------|--------------|
| Beam | ω_{PB}/ω_{CB} | 0.3 |
| | $\gamma_B = E_B/m_0c^2$ | 9.0 |
| Plasma | ω_{PP}/ω_{CP} | 0.1-1.9 |
| | v_{TH}/c | 0.0, 0.002, |
| | | 0.0044, 0.01 |
| Wave | $l = k_y V_B/\omega_{CB}$ | 6-20 |
| | $k_x c/\omega_{CB}$ | 0-10000 |

Table 2 shows the range of parameters of the dispersion equation that was studied. The value of the normalized plasma electron thermal velocity, v_{TH}/c , is approximately equivalent to thermal energies of 0, 1, 5 and 25 eV, respectively.

Extraordinary normal modes—Maxwellian plasma

Since the plasma normal modes play a basic role in the beam-plasma interaction, discussion of their characteristics is presented before those of the instability. Figure 3, we recall, shows a typical plot of the normal modes for a cold plasma at a given plasma density. For the hybrid branch (lower branch), the asymptotic value of frequency in the large wave number region is the hybrid frequency.

In Fig. 6, the extraordinary normal modes of a 1 eV Maxwellian plasma are presented. Specifically, the frequency of the normal mode, ω_k/ω_{CB} , is plotted vs the wave number of the mode, $k_{\perp}c/\omega_{CB}$, with plasma frequency, ω_{PP}/ω_{CP} , as a parameter. The first (hybrid) and second branch of the plasma normal modes are given. The main feature of the hybrid branch is that the frequency for large wave number is asymptotic to the plasma electron cyclotron frequency instead of the hybrid frequency as in the cold plasma case. For plasma densities below $\omega_{PP}/\omega_{CP} = 1.7$, thermal effects are negligible for wave numbers $k_{\perp}c/\omega_{CB} < 100$. Thus, from this figure, one would expect the unstable mode to be affected by thermal properties of the plasma only for wavelengths such that $k_{\perp}c/\omega_{CB} \geq 1000$, for a 1 eV plasma for $\omega_{PP}/\omega_{CP} \leq 1.5$. We also note, that after the plasma density surpasses the hybrid density for a given frequency of the normal mode (given beam harmonic) there exists two points in the wave number spectrum for the same frequency. That is, a given beam harmonic will exhibit exact resonance between the beam and plasma

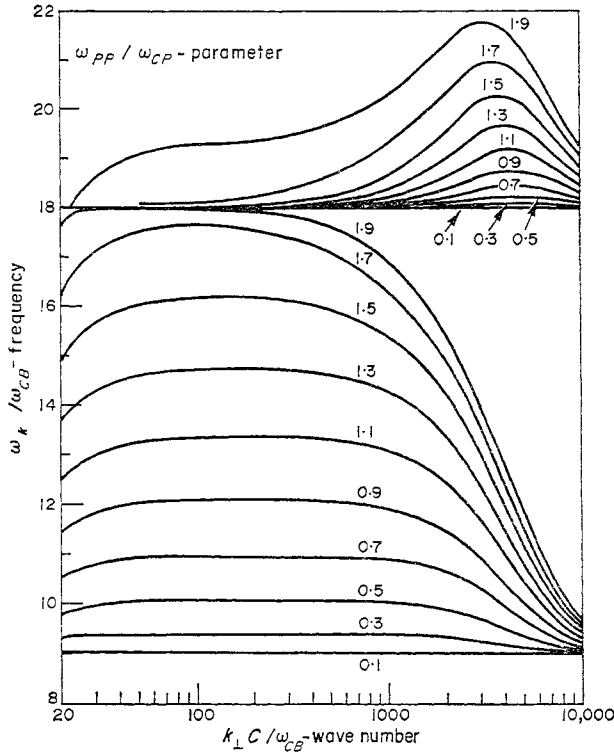


FIG. 6.—Extraordinary normal modes of a Maxwellian plasma at 1 eV.

mode at two values of wave number when the plasma density is greater than the hybrid density for that harmonic. Hence, near these two exact beam-plasma resonances we expect enhanced growth rates. As an example, let us consider the $l = 12$ ($\omega_k/\omega_{CB} = 12$) beam harmonic. We note that the hybrid density for this harmonic for a beam of $\gamma_B = 9.0$ is given by $\omega_{PP}^*/\omega_{CP} = 0.882$, from Table 1. From Fig. 6, we see for $\omega_{PP}/\omega_{CP} = 0.9$ that exact resonance occurs at about $k_{\perp}c/\omega_{CB} = 100$ and 800. Thus near these values we expect peaking of the beam-plasma growth rate. At $\omega_{PP}/\omega_{CP} = 1.1$, peaking should occur near $k_{\perp}c/\omega_{CB} = 16.5$ and 2500.

Besides interaction with the first branch there will exist interaction at frequencies near the second multiple of the plasma electron cyclotron frequency. These modes possess a feature unlike the first branch in that there is a distinct peak in the frequency-wave number spectrum, whereas, for the first branch, a wide plateau exists. This gives rise to no beam-plasma interaction for low values of wave number, then a region of interaction, then again no interaction at higher values. These modes are asymptotic to the second multiple of the plasma electron cyclotron frequency at large wave number. For the beam parameters mentioned above, we observe from the plot that for $l = 19$, exact beam-plasma mode resonance occurs for $\omega_{PP}/\omega_{CP} \geq 1.0$, moreover, for $\omega_{PP}/\omega_{CP} = 1.1$, exact resonance occurs near $k_{\perp}c/\omega_{CB} = 3000$ and 6000. This represents the region in wavelength space where strongest beam-plasma interaction is expected with lesser interaction occurring for wavelengths above or below this region.

The features for a 5 and 25 eV plasma are similar to the 1 eV case discussed above.

The main difference is the shift in the normal mode curves with increasing temperature to lower values of wave number or to longer wavelengths. This implies that unstable modes at 1 eV may become stable at a higher temperature. This and the other features indicated above will emerge when the stability analysis is presented.

Beam-plasma unstable mode

The results of the beam-plasma interaction for the range of parameters of Table 2 are presented as a function of beam harmonic at a given plasma density. That is, at a given plasma density, ω_{PP}/ω_{CP} , the growth rate at each unstable beam harmonic, l , is presented. The effect of plasma temperature on these unstable modes is also shown.

In Figs. 7–11, results of the unstable beam-plasma mode are plotted in such a manner that a clear comparison can be made with the experimental results of Astron. Specifically, for a given set of plasma parameters, density (ω_{PP}/ω_{CP}) and temperature (KT_P), the growth rate versus wave number of the unstable beam harmonics is plotted. They are presented in the order of increasing plasma density and temperature.

In Fig. 7, the results are shown for a plasma density of $\omega_{PP}/\omega_{CP} = 0.1$. In the cold plasma case, the growth rate of the unstable mode reaches a saturated level at relatively low wave numbers ($k_{\perp}c/\omega_{CB} \sim 50$) and remains at that level for larger wave numbers. This is the region where the analytical results of the cold beam-cold plasma model are especially applicable. When the plasma temperature reaches 1 eV, the growth rate departs from the cold plasma results in the large wave number region ($k_{\perp}c/\omega_{CB} > 500$), as shown by the right-hand portion of the bottom graph in Fig. 7. Although subsequent results are presented in the same manner, only plasma temperatures of 0 and 1 eV are shown.

For a cold plasma of density $\omega_{PP}/\omega_{CP} = 0.1$, Fig. 7 also indicates that only beam harmonics $l \leq 9$ are unstable, with the $l = 9$ harmonic being the most unstable for $k_{\perp}c/\omega_{CB} > 10$. This is reasonable since the plasma normal mode at this plasma density and in this wave number region is located just above the plasma electron cyclotron frequency, $\omega_{CP} = 9\omega_{CB}$. As the plasma temperature increases to 1 eV, the growth rates at these harmonics begin to decrease at large wave numbers (> 500). Also, at finite plasma temperature, beam-plasma interaction begins to occur at the $l = 18$ beam harmonic, due to the second branch of the plasma normal modes which lie above the second plasma electron cyclotron frequency, $2\omega_{CP} = 18\omega_{CB}$. The strength of the interaction at the $l = 9$ and 18 harmonics is very similar for $k_{\perp}c/\omega_{CB} \geq 6000$, while the $l \leq 8$ harmonics have already become stable in this wave number region. Thus, for waves in Astron having wavelengths of $k_{\perp}c/\omega_{CB} \geq 6000$, these results indicate that only the $l = 9$ and 18 beam harmonics are unstable at this plasma density and temperature.

As plasma temperature increases, the stabilized region of wavelengths becomes larger by shifting towards long wavelength oscillations. Finally, if the plasma temperature increased to 25 eV, all waves for $k_{\perp}c/\omega_{CB} \geq 6000$ are stabilized at all beam harmonics, as indicated in the top graph of Fig. 7.

Figure 8 shows the results for a plasma density of $\omega_{PP}/\omega_{CP} = 0.3$. For the case of a cold plasma, the results indicate that beam harmonics $l \leq 10$ are unstable. The interaction becomes stronger at harmonics $l \leq 9$ for this plasma density, while at the $l = 10$ harmonic, interaction has just begun to occur (see Fig. 4). When a finite plasma temperature is included (1 eV), the unstable modes begin to stabilize as before,

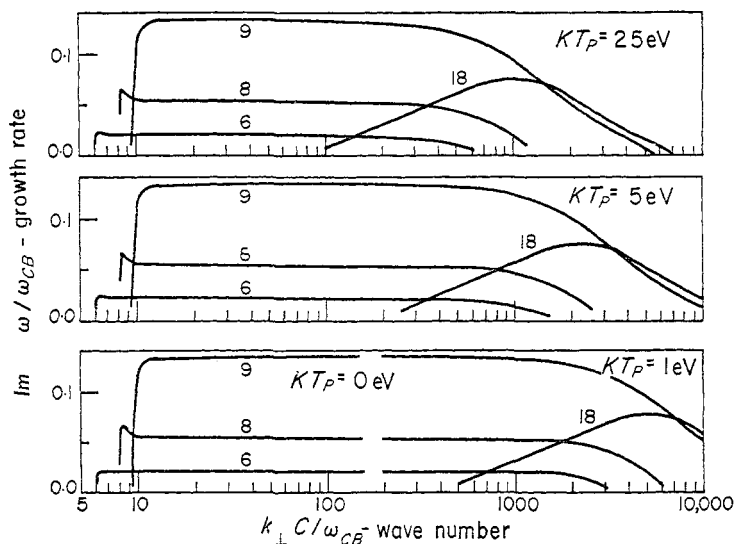


FIG. 7.—Growth rate vs wave number for a Maxwellian plasma at plasma density; $\omega_{PP}/\omega_{CP} = 0.1$.

at large wave numbers and become completely stable at high enough wave numbers. At this plasma density, plasma thermal effects initiate unstable oscillations at beam harmonics $l = 14-18$, due to beam-second branch interaction. These unstable modes persist for only a limited range of wavelengths. The interaction strength with the second branch of the plasma modes is greatest at the $l = 18$ harmonic and decreases progressively for lower beam harmonics. If the plasma temperature were 25 eV, only the $l = 9$ and 18 harmonics are unstable for waves with $k_{\perp} c / \omega_{CB} > 4000$, with these harmonics becoming stable for $k_{\perp} c / \omega_{CB} > 12-15 \times 10^3$.

Figure 9 is for a plasma density of $\omega_{PP}/\omega_{CP} = 0.5$. This reveals that the beam-hybrid mode interaction occurs for beam harmonics $l \leq 10$, and for beam-second branch interaction at $l = 12-18$. Plasma thermal effects are largest for those harmonics whose numbers are above multiples of the plasma electron cyclotron frequency, i.e. $\omega_{CP}, 2\omega_{CP}, 3\omega_{CP}, \dots$, and interacting with the branch of the normal modes

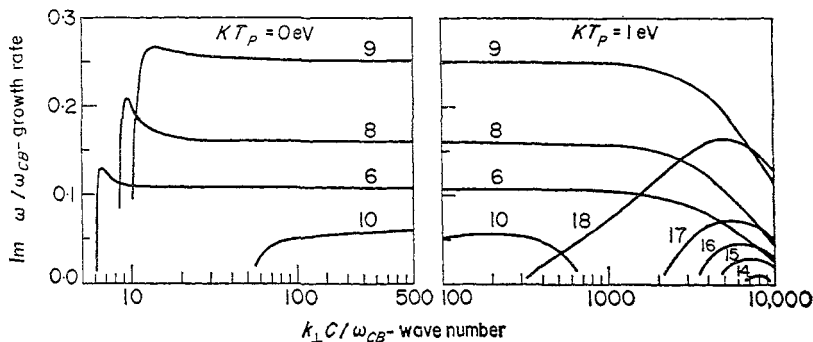


FIG. 8.—Growth rate vs wave number for a Maxwellian plasma at plasma density; $\omega_{PP}/\omega_{CP} = 0.3$.

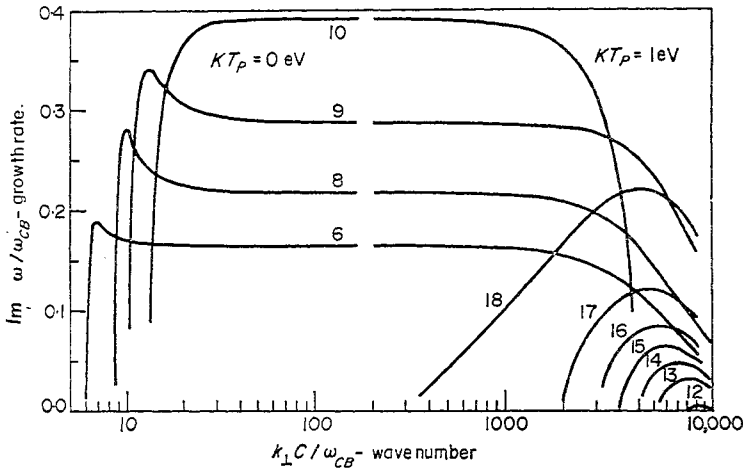


FIG. 9.—Growth rate vs wave number for a Maxwellian plasma at plasma density; $\omega_{PP}/\omega_{CP} = 0.5$.

which lies above the respective plasma electron cyclotron frequency. For the case presented in Fig. 9, this is only the $l = 10$ beam harmonic. Other plasma temperature effects are as indicated in previous discussions.

When plasma density reaches a value of $\omega_{PP}/\omega_{CP} = 0.7$ (Fig. 10), beam harmonics $l \leq 12$ begin to interact with the hybrid branch, while harmonics $l = 12-19$ become unstable due to interaction with the second plasma branch. As the graphs indicate, this plasma density is approximately the density for the onset of beam-second branch interaction with harmonics above the second plasma electron cyclotron frequency, $2\omega_{CP}$, i.e. $l = 19$. We might also note the local peaking of the $l = 10$ unstable mode for a 1 eV plasma near $k_{\perp} c / \omega_{CB} = 2700$, which is due to beam-plasma

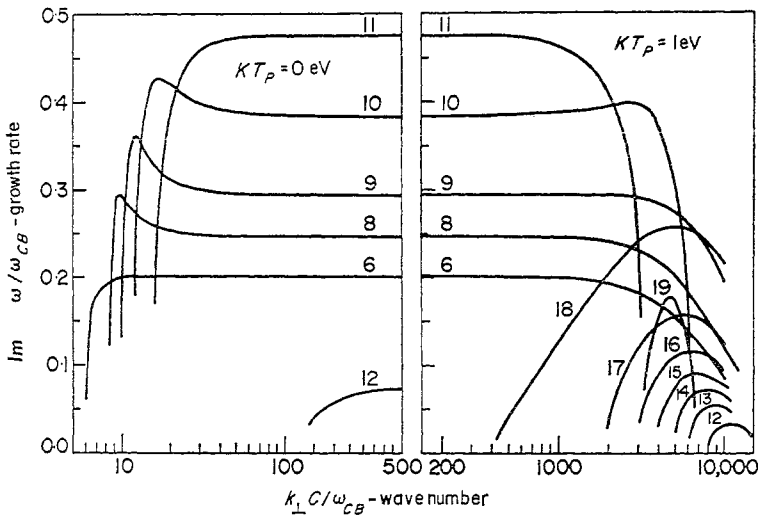


FIG. 10.—Growth rate vs wave number for a Maxwellian plasma at plasma density; $\omega_{PP}/\omega_{CP} = 0.7$.

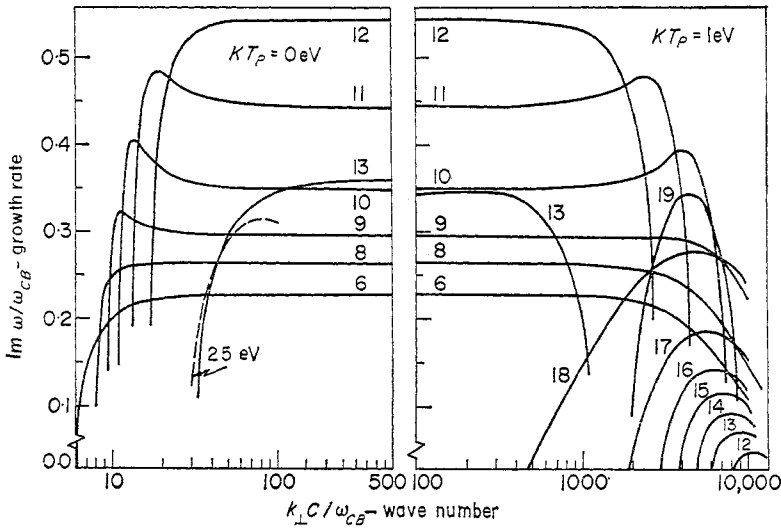


FIG. 11.—Growth rate vs wave number for a Maxwellian plasma at plasma density; $\omega_{PP}/\omega_{CP} = 0.9$.

resonance effects. Upon further increase in plasma density ($\omega_{PP}/\omega_{CP} = 0.9$, Fig. 11), more beam harmonics become unstable as a result of interaction with a given plasma mode branch.

We have thus far discussed the growth rate characteristics as a function of plasma density. We now summarize some of the general features of these results at a given beam harmonic. In general, a given beam harmonic interacts with any plasma normal mode; however, the interaction is strongest with that plasma mode in the immediate vicinity of the harmonic. There is an onset condition, $\omega_P > (\omega_P)_{onset}$, for these interactions. Relative to this onset criteria, Table 3 shows the plasma density required for a given beam harmonic to interact with a given plasma normal mode. In our model, the interaction can occur with the hybrid mode (first branch) or the second branch (above the second plasma electron cyclotron frequency), in the case of a plasma with finite temperature. These densities are not very exact, but they do reflect the above statements.

The plasma system of interest is one in which the plasma density increases from an initially low value. On the basis of our analysis one expects to see interaction at $l = 9$ and $l = 18$ beam harmonics at relatively low plasma densities. As the density increases, the harmonics below the normal modes become unstable; that is, the $l = 8, 7, 6, \dots$ beam harmonics appear progressively unstable as a result of interaction with the hybrid branch, and the $l = 17, 16, 15, \dots$ beam harmonics as a result of interaction with the second branch. Upon further increase in plasma density, beam harmonics above the first and second plasma electron cyclotron frequency (ω_{CP} and $2\omega_{CP}$) become unstable due to interaction with the plasma mode in that region. When the plasma density reaches a value where resonance between a given beam harmonic and the plasma mode occurs, the interaction becomes relatively strong. In general, whenever a beam-plasma mode resonance occurs, a local, if not absolute, maximum in the growth rate appears. This effect can be seen in Fig. 4 for beam harmonics interacting with the first plasma mode branch. The growth rate at a given

TABLE 3. ESTIMATE OF THRESHOLD PLASMA DENSITY FOR THE UNSTABLE BEAM-PLASMA MODE AS A FUNCTION OF PLASMA MODE BRANCH

| l | $(\omega_{PP}/\omega_{CP})_{\text{onset}}$ | |
|-----|--|---------------|
| | Hybrid branch | Second branch |
| 6 | 0.083* | — |
| 8 | 0.051* | — |
| 9 | 0.000 | — |
| 10 | 0.30 | 2.00 |
| 11 | 0.52 | 1.00 |
| 12 | 0.70 | 0.50 |
| 13 | 0.87 | 0.42 |
| 14 | 1.00 | 0.30 |
| 15 | 1.15 | 0.25 |
| 16 | 1.30 | 0.20 |
| 17 | 1.50 | 0.12 |
| 18 | 1.60 | 0.08 |
| 19 | 1.70 | 0.70 |
| 20 | 1.90 | 1.10 |

* From Table 1.

beam harmonic saturates with further increase in plasma density, since a tradeoff between mode proximity to a given harmonic, $\omega_k - l\omega_{CB}$, and the strength of the mode ω_{PP} and ϵ_y , become counteracting influences. This saturated level is approached from either above or below depending on the beam harmonic and the magnitude of this level depends on beam parameters, as given in equation (24).

In addition to initiating beam-plasma interaction at multiples of the plasma electron cyclotron frequency, the effect of increasing plasma temperature is to shift the unstable spectrum to longer wavelengths. That is, for a given plasma temperature, there are regions of the wave number spectrum which are unstable but separated by stable regions. The first unstable region, in general, represents interaction with the hybrid normal mode while the second unstable region is the result of interaction with the second branch of the plasma normal modes. At higher plasma temperatures, these regions shift towards lower wave numbers and also decrease in width. It must be noted that plasma temperature does not substantially affect the relative magnitudes of the growth rates at any given plasma density.

We turn now to the wavelength region for which $k_{\perp}c/\omega_{CB} \geq 100$, and observe that harmonics below the plasma electron cyclotron frequency ($l < 9$) interact with only the hybrid mode. Resonance never occurs between the beam and plasma mode for these harmonics, in the wavelength region cited above. For these harmonics, the frequency of the unstable mode is essentially coincident with the beam harmonic and does not vary as a function of plasma density or growth rate of the unstable mode. An identical situation occurs for those harmonics below the second plasma electron cyclotron frequency ($l < 18$) when interacting with the second branch of the plasma normal modes. That is, the location of the frequency of the unstable mode lies approximately at the beam harmonic. The same situation also occurs when the plasma density greatly exceeds the hybrid density for a given beam harmonic, i.e. when the frequency of the plasma normal mode, ω_k , is much greater than the beam harmonic frequency, $l\omega_{CB}$. This occurs for $l = 10$, at plasma densities greater than $\omega_{PP}/\omega_{CP} = 1.1$, for a cold plasma. In short, the results indicate that when the plasma normal mode is far from the beam harmonic, yet an unstable interaction

exists, the location of the unstable mode is coincident with the beam harmonic, i.e. $Re \omega/\omega_{CB} \cong l$.

When the plasma normal mode is in the vicinity of the beam harmonic, that is, near resonance, we see that the location of the unstable mode, $Re \omega/\omega_{CB}$, is relatively far from the beam harmonic. This same situation also occurs when the growth rate rapidly decreases towards zero due to plasma thermal properties. These two cases are much the same since beam-plasma resonance does occur just prior to the rapid decrease in the growth rate, because the warm plasma normal modes are asymptotic to multiples of the plasma electron cyclotron frequency, and there are two values of wave number for resonance.

In the previous section mention was made of the restrictions on wavelengths which render this investigation applicable to the physical system under consideration. This corresponds to the region for the cold plasma where the normal modes reach an asymptotic frequency, i.e. the upper hybrid frequency, and the growth rates approach a constant value independent of wave number. Also consistent with the equations employed in this analysis, the Debye length will be taken as the lower limit on the wavelengths of interest. This, along with the upper bound mentioned above, will provide the region of applicability of the present theory to finite systems.

Comparison of theory and experiment

Taking into account the upper and lower limits on the wavelengths, the model and subsequent results indicate the following for the beam-plasma interaction in the Astron system. Table 4 lists those beam harmonics from Figs. 7-11 which are unstable with respect to interaction with the hybrid or the second branch of the plasma normal modes. This means, that somewhere in the restricted region of wave number space, these beam harmonics undergo unstable interaction. Some of these harmonics indicate instability for the entire region, while others are unstable for only a limited region of the allowable wave number space. They are tabulated in order of descending growth rate or degree of beam-plasma interaction.

As an example, at $\omega_{PP}/\omega_{CP} = 0.1$, beam harmonics $l = 5-9$ display unstable oscillations via interaction with the hybrid branch of the plasma normal modes. The $l = 9$ harmonic has the greatest growth rate with the subsequent harmonics having progressively less interaction. Only the $l = 18$ beam harmonic is unstable with respect to interaction with the second branch of the normal modes. These unstable harmonics do appear in the allowable wavelength region regardless of plasma temperature, though their growth rate may decrease depending on plasma temperature. In some cases, a beam harmonic may be completely stabilized at a plasma temperature of 25 eV.

TABLE 4. UNSTABLE BEAM HARMONICS IN THE ALLOWABLE WAVE NUMBER REGION AS A FUNCTION OF PLASMA PARAMETERS

| ω_{PP}/ω_{CP} | Hybrid branch | Second branch |
|---------------------------|-------------------------------|-------------------------|
| 0.1 | 9, 8, 7, 6, 5 | 18 |
| 0.3 | 9, 8, 7, 6, ..., 10, ..., 1 | 18, 17, 16, 15, 14 |
| 0.5 | 10, 9, 8, ..., 1 | 18, 17, ..., 12 |
| 0.7 | 11, 10, 9, 8, ..., 12, ..., 1 | 18, 19, 17, 16, ..., 12 |
| 0.9 | 12, 11, 10, 13, 9, 8, ..., 1 | 19, 18, 17, ..., 12 |

Experiments in Astron, relative to the "hybrid" mode, have produced the following observations (FESSENDEN *et al.*, 1970). R.f. radiation has been observed at beam harmonics between the plasma electron cyclotron frequency and the upper hybrid frequency, and at harmonics near subsequent integral multiples of the plasma electron cyclotron frequency. This radiation is an integrated radiation over the time of the experiment. During this time the plasma density increases from zero to some finite value, which implies that the upper hybrid frequency also increases with time. The integrated r.f. radiation appears to be largest at the beam harmonic closest to the plasma electron cyclotron frequency and decreases at progressively higher harmonics, up to the harmonic just below the largest hybrid frequency (largest plasma density) reached during the experiment. These harmonics progressively appear unstable, then stable, as the experiment evolves in time.

Comparing these experimental results to those tabulated in Table 4 and shown in Figs. 7-11, we see that oscillations at harmonics above the plasma electron cyclotron frequency, for interaction with the hybrid mode, are indeed unstable, with more harmonics becoming unstable as the plasma density increases. Similar features occur above the second plasma electron cyclotron frequency for interaction with the second branch. Our model, however, predicts two additional results which are not experimentally observed. The first is that there are harmonics below the electron cyclotron frequency that are also unstable; that is, $l \leq 8$ for interaction with the hybrid mode and $l = 12-17$ for interaction with the second branch. The second is that for the plasma temperatures probably attained in the experiments, our results might not indicate stabilization of all beam harmonics. We may, therefore, conclude that other physical mechanisms not presently contained in our analysis might be responsible for the apparent disagreement.

Two effects which exist in Astron, and not contained in our model thus far, are collisions between plasma electrons and neutral particles and energy spread of beam particles. In Astron, we recall that the plasma is formed by ionization of a background gas. Thus, the particles of the plasma are most likely to collide with the neutral particles because of the relatively high density of the latter. Also, beam particles injected into the plasma region possess a spectrum in velocities, thus giving rise to an energy spread about a monoenergetic distribution. These two effects will be treated in the next two sections.

Convective nature of the unstable mode

Before concluding this section, it would be desirable to assess the extent to which the results predicted by this analysis can be observed in Astron. We do this by estimating the time it takes the unstable mode to convect across the lateral dimension of the system.

Assuming this appropriate dimension to be the *E*-Layer thickness, t_{EL} , the time it takes the wave to leave the Astron region (where our model is expected to apply) is given by

$$T = \frac{t_{EL}}{\partial\omega_R/\partial k_x}, \quad (33)$$

where $\partial\omega_R/\partial k_x$ is the group velocity of the unstable mode in the direction

perpendicular to the beam. The time in which the unstable wave grows is

$$T_I = \frac{1}{\omega_I} \quad (34)$$

where ω_I is the growth rate. If the instability is to be observed, then the following condition must be satisfied,

$$T_I \ll T. \quad (35)$$

In order to get an order of magnitude for these times with respect to the present model, we let $T_I \sim T$ in equation (35) and obtain an approximate upper bound on the group velocity of the unstable modes, i.e.

$$\frac{1}{\omega_I} = \frac{t_{EL}}{(\partial\omega_R/\partial k_x)_{\max}} \quad (36)$$

or

$$\left(\frac{\partial\omega_R}{\partial k_x}\right)_{\max} = t_{EL}\omega_I.$$

Normalizing the various quantities to previous variables, we obtain

$$\left[\frac{\partial(\omega_R/\omega_{CB})}{\partial(k_x c/\omega_{CB})}\right]_{\max} = \frac{t_{EL}}{R} \left(\frac{\omega_I}{\omega_{CB}}\right), \quad (37)$$

which for Astron becomes

$$\left[\frac{\partial(\omega_R/\omega_{CB})}{\partial(k_x c/\omega_{CB})}\right]_{\max} \cong \frac{1}{2} \left(\frac{\omega_I}{\omega_{CB}}\right). \quad (38)$$

If the value of $\partial\omega_R/\partial k_x$ as obtained from our numerical results is less than the value given above, one might conclude that these modes will be observed in Astron.

From previous considerations we restrict ourselves to beam harmonics above the plasma electron cyclotron frequency ($l \geq 9$) and their interaction with the hybrid mode only. Similar results can be obtained for beam harmonics $l \geq 18$, and their interaction with the second branch. The first group represents the fastest convecting modes since it can be shown that they have the largest group velocity. Substituting the corresponding parameters in equation (38), we find that

$$\frac{\left(\frac{\partial\omega_R/\omega_{CB}}{\partial k_x c/\omega_{CB}}\right)}{\omega_I/\omega_{CB}} < 0.001,$$

which clearly indicates that the wave grows substantially before it can convect out of the system.

4. COLLISIONAL EFFECTS

A process that is not included in our base model is collisions between the plasma particles (electrons) and the dense neutral background gas. Generally, collisions tend to act as a damping mechanism of the plasma normal modes, therefore, we postulate that they will tend to stabilize the unstable beam-plasma interactions. In this section, an analytical treatment is carried out on a model that includes the effect of collisions.

Because of applicability to Astron, we restrict our analysis to oscillations with short wavelengths perpendicular to the beam propagation direction, as given by equation (17) and (18). It has already been noted that at relatively low plasma densities the strongest interaction occurs at those beam harmonics which interact with the hybrid normal mode. Thus, we consider a cold plasma model where collisions among plasma particles are ignored, but collisions between plasma and neutral particles are included. These assumptions seem especially meaningful to Astron, since the plasma is formed by ionization of a neutral gas.

We consider again the response of a beam and plasma species to an arbitrary electromagnetic plane wave with time and space variation given in equation (1). The resulting wave equation is given by equation (3). The beam species is identical to that used previously. The basic equations describing these particles are given by equation (5), with the resulting perturbed current density shown in equation (8).

In addition to the assumptions used in the cold plasma case, the plasma particles are assumed to have collisions with the background neutral particles. The relevant equations are given by;

$$\begin{aligned} \frac{\partial n_\alpha}{\partial t} + \nabla \cdot n_\alpha \mathbf{v}_\alpha &= 0 \\ m_\alpha \frac{d\mathbf{v}_\alpha}{dt} &= q_\alpha \left[\mathbf{E} + \frac{1}{c} \mathbf{v} \times \mathbf{B} \right] - \nu_{\alpha N} m_\alpha \mathbf{v}_\alpha \\ \mathbf{J}_\alpha &= n_\alpha q_\alpha \mathbf{v}_\alpha, \quad \frac{d}{dt} = \frac{\partial}{\partial t} + \mathbf{v}_\alpha \cdot \nabla. \end{aligned} \quad (39)$$

Here, $\nu_{\alpha N}$ is the collision frequency between the plasma species α and the neutral particles of the system, and the other quantities are as defined previously. The perturbed current density in the plasma now becomes

$$\frac{4\pi i\omega}{c^2} \mathbf{J}_{1P} = - \frac{\omega_{PP}^2}{c^2 [(\omega + i\nu_{EN})^2 - \omega_{CP}^2]} \left\{ \omega(\omega + i\nu_{EN}) \boldsymbol{\epsilon} - i\omega\omega_{CP} \boldsymbol{\times} \boldsymbol{\epsilon} - \frac{\omega(\omega_{CP} \cdot \boldsymbol{\epsilon})}{\omega + i\nu_{EN}} \boldsymbol{\omega}_{CP} \right\}. \quad (40)$$

Combining the perturbed current densities and inserting into the wave equation we obtain the following dispersion equation for the extraordinary mode;

$$\begin{aligned} & \left[-k_y^2 c^2 + \omega^2 - \omega_{PB}^2 - \frac{\omega(\omega + i\nu_{EN})\omega_{PP}^2}{(\omega + i\nu_{EN})^2 - \omega_{CP}^2} \right] \\ & \times \left[-k_x^2 c^2 + \omega^2 - \omega_{PB}^2 \frac{\omega^2/\gamma_B^2 + k_x^2 V_B^2}{(\omega - k_y V_B)^2} - \frac{\omega(\omega + i\nu_{EN})\omega_{PP}^2}{(\omega + i\nu_{EN})^2 - \omega_{CP}^2} \right] \\ & - \left[k_x k_y c^2 - \frac{i\omega\omega_{CP}\omega_{PP}^2}{(\omega + i\nu_{EN})^2 - \omega_{CP}^2} - \omega_{PB}^2 \frac{k_x V_B}{\omega - k_y V_B} \right] \\ & \times \left[k_x k_y c^2 + \frac{i\omega\omega_{CP}\omega_{PP}^2}{(\omega + i\nu_{EN})^2 - \omega_{CP}^2} - \omega_{PB}^2 \frac{k_x V_B}{\omega - k_y V_B} \right] = 0. \end{aligned} \quad (41)$$

This equation reduces to equation (13) in the limit of no collisions.

Before solving this equation, we consider the cold plasma dispersion equation in the large $k_x c$ limit. In equation (41) we let the beam density be zero and in the absence of collisions we find that the frequency of oscillation is at the upper hybrid frequency. Assuming this frequency to be the same when collisions are included, and the collision frequency ν_{EN} to be much less than the upper hybrid frequency, one finds that the plasma oscillations become damped, as shown by

$$\omega \cong \omega_H - i\nu_{EN} \left(1 - \frac{1}{2} \frac{\omega_{PP}^2}{\omega_H^2} \right). \tag{42}$$

Since these plasma modes are damped by collisions in the short wavelength region, it is possible that collisions may have their greatest effect on the beam-plasma unstable mode in the vicinity of the upper hybrid frequency.

We return to equation (41) and consider the region of large $k_x c$. The resulting equation is

$$\begin{aligned} & \{ \omega [(\omega + i\nu_{EN})^2 - \omega_{CP}^2] - (\omega + i\nu_{EN}) \omega_{PP}^2 \} (\omega - k_y V_B)^2 - \frac{\omega_{PB}^2}{\gamma_B^2} \\ & \times \{ \omega [(\omega + i\nu_{EN})^2 - \omega_{CP}^2] + (\gamma_B^2 - 1) (\omega + i\nu_{EN}) \omega_{PP}^2 \} \cong 0. \end{aligned} \tag{43}$$

Recalling the periodicity of the system in the beam direction, i.e.

$$k_y V_B = l \omega_{CB},$$

we find that the beam-plasma mode with collisional effects can be described by a third order equation in ω , with the unstable mode being located near the beam harmonics. To lowest order we wish to know the sign of the quantity,

$$\frac{\partial \text{Im } \omega}{\partial \nu} \Big|_{\nu=0}, \tag{44}$$

where $\text{Im } \omega/\nu = 0$ is the growth rate for zero collision frequency. If the sign of the quantity in equation (44) is positive, then collisions have a de-stabilizing effect at low collision frequencies, whereas, if it is negative, collisions provide a stabilizing effect on the beam-plasma unstable mode. These effects are calculated for the same regions of plasma density considered in the Cold Beam-Cold Plasma Model, i.e. at densities corresponding to resonance and non-resonance between beam harmonic and the upper hybrid frequency.

Beam-plasma resonance

In the case of resonance, as given in equation (25), the growth rate to lowest order in collision effects is

$$\text{Im } \frac{\omega}{\omega_{CB}} \cong \frac{\sqrt{3}}{2} \left[\frac{\omega_{PB}^2 l^2 - \gamma_B^2}{\omega_{CB}^2 2l} \right]^{1/3} - \frac{\gamma_B \nu_{EN} l^2 + \gamma_B^2}{3 \omega_{CP} 2l^2}, \tag{45}$$

which for $\nu_{EN} = 0$, reduces to equation (26). From this we see that collisions have a stabilizing effect on the beam-plasma unstable mode at exact resonance. We recall, that at this beam-plasma resonance, one observes almost maximum growth rate for the entire range of plasma densities at a given beam harmonic. We might therefore

TABLE 5. COLLISION FREQUENCY, ν_{EN} , REQUIRED TO STABILIZE THE BEAM-PLASMA MODE AT EXACT RESONANCE

| l | ν_{EN}/ω_{CB} |
|-----|------------------------|
| 10 | 1.26 |
| 11 | 1.70 |
| 12 | 2.06 |
| 13 | 2.36 |

infer that collisions have their largest effect where the interaction is the strongest. This perhaps is expected since the greatest damping of the plasma mode occurs at the oscillation frequency which coincides with the beam harmonic.

Though it is not meaningful to discuss complete stabilization due to collisions in the present analysis one can at least obtain some feeling for the magnitude of the collision frequency required to stabilize the mode at beam-plasma resonance. Table 5 lists the collision frequency required for the growth rate of equation (45) to become zero for Astron parameters. We see that collision frequencies of the order of the beam cyclotron frequency could stabilize the beam-plasma interaction at exact resonance.

Non beam-plasma resonance

For the case when the plasma density is such that resonance between the plasma normal mode and a given beam harmonic does not occur, we might expect less damping due to collisions. The growth rate for this density region, to lowest order in the collision frequency, is

$$\begin{aligned} \text{Im} \frac{\omega}{\omega_{CB}} \cong & \frac{1}{\gamma_B} \frac{\omega_{PB}}{\omega_{CB}} \left[\frac{l^2 - \gamma_B^2(1 + \omega_{PP}^2/\omega_{CP}^2) + \gamma_B^4\omega_{PP}^2/\omega_{CP}^2}{\gamma_B^2(1 + \omega_{PP}^2/\omega_{CP}^2) - l^2} \right]^{1/2} \\ & + \frac{\gamma_B}{2} \frac{\nu_{EN}}{\omega_{CP}} \frac{\omega_{PB}^2}{\omega_{CB}^2} \frac{\gamma_B^2\omega_{PP}^2}{l^2\omega_{CP}^2} \\ & \times \frac{4l^2(l^2 + \gamma_B^2) - (l^2 - \gamma_B^2)[l^2 - \gamma_B^2(1 + \omega_{PP}^2/\omega_{CP}^2)]}{[l^2 - \gamma_B^2(1 + \omega_{PP}^2/\omega_{CP}^2)]^3}, \quad (46) \end{aligned}$$

where we have assumed that

$$\gamma_B^2(1 + \omega_{PP}^2/\omega_{CP}^2) - l^2 > 0$$

and

$$l^2 - \gamma_B^2(1 + \omega_{PP}^2/\omega_{CP}^2) + \gamma_B^4\omega_{PP}^2/\omega_{CP}^2 \geq 0$$

for instability to occur in the limit of zero collision frequency. This result agrees with equation (22) in the $\nu_{EN} = 0$ limit. As in that case, we consider two groups of beam harmonics; those equal to and above the plasma electron cyclotron frequency, $l \geq \gamma_B$, and those below, $l < \gamma_B$.

For beam harmonics above the plasma electron cyclotron frequency, we see that the collision term is negative and thus collisions have a stabilizing effect on these harmonics. For beam harmonics below the plasma electron cyclotron frequency, the results indicate that collisions have a stabilizing influence only for plasma densities up to a critical value given by

$$\frac{\bar{\omega}_{PP}^2}{\omega_{CP}^2} = \frac{4l^2(l^2 + \gamma_B^2) - (\gamma_B^2 - l^2)^2}{\gamma_B^2(\gamma_B^2 - l^2)}, \quad (47)$$

TABLE 6. CRITICAL PLASMA DENSITY INCLUDING COLLISIONAL EFFECTS FOR BEAM HARMONICS $l < \gamma_B$. SEE EQUATION (47)

| l | $\bar{\omega}_{PP}/\omega_{CP}$ |
|-----|---------------------------------|
| 8 | 5.17 |
| 7 | 3.07 |
| 6 | 2.02 |
| 5 | 1.28 |
| 4 | 0.61 |
| 3 | 0.00 |
| 2 | 0.00 |
| 1 | 0.00 |

and a de-stabilizing effect for plasma densities above this value. Table 6 gives the value of this critical density for Astron parameters; and we note, for example, that the $l = 8$ beam harmonic experiences a stabilizing effect due to collisions for plasma densities up to $\omega_{PP}/\omega_{CP} = 5.17$, and a destabilizing effect for densities above this value. It is interesting also to note that collisions have a destabilizing effect at all plasma densities for beam harmonics less than three.

In this case of non-resonance the effect of collisions is of order $(\nu_{EN}/\omega_{CP})(\omega_{PB}/\omega_{CB})$ less than the zero collision growth rate, that is, it is two orders of magnitude less, while in the hybrid density case, the effect is approximately of the same order as the $\nu_{EN} = 0$ growth rate. This may be viewed as further confirmation of the fact that collisional effects are most dominant when the plasma normal mode is near a giving beam harmonic.

From the above statement, we might expect that the onset condition for instability for beam harmonics above the plasma electron cyclotron frequency to be greatly affected by collisions. In the zero collision case, the onset condition is given by equation (27), and the following result is obtained at that plasma density;

$$\left. \frac{\partial \text{Im } \omega/\omega_{CB}}{\partial(\gamma_B \nu_{EN}/3\omega_{CP})} \right|_{\nu_{EN}=0} \cong -\frac{l^2 + \gamma_B^2}{2l^2}. \quad (48)$$

This states that the damping due to collisions at the onset condition is approximately the same as that at the hybrid density, which implies that collisions have a tendency to increase the threshold plasma density for beam harmonics above the plasma electron cyclotron frequency.

In Appendix A, we show that the dispersion equation for the Cold Beam-Cold Plasma model in the large wave number region is similar to that of the streaming instability. The effects of collisions on the streaming instability have been examined by BÖHMER *et al.* (1971) and SINGHAUS (1964), among others. These two references show the enhancement of growth rate at low frequencies (Table 6, $l \leq 3$), and reduction of growth rate in the region of the plasma modes. Our results reduce to those obtained by these authors in the appropriate limits.

5. EFFECTS OF BEAM ENERGY SPREAD

A feature of the beam particles in Astron that is not included in our base model is that the beam particles have a finite distribution in streaming energy. The purpose of this section is to examine the effect of this energy spread on the beam-plasma unstable

mode. It is not our intent to imply that the streaming energy spread is in any way the most dominant form of energy spread relative to the beam-plasma mode. The point is that the streaming energy spread is a consequence of the Astron injection system. The plasma species, wave vectors and model geometry are the same as in Section 2.

We employ the same beam model used before but with the addition of a spread in particle energy or velocity. The appropriate equations are the relativistic Vlasov equations which we choose to write in Minkowski space (SUDAN, 1965), i.e.

$$\frac{\partial f}{\partial t}(\mathbf{x}, \mathbf{u}, t) + \frac{c}{\gamma} \mathbf{u} \cdot \frac{\partial f}{\partial \mathbf{x}} + \frac{q}{m_0 c} \left[\mathbf{E}(\mathbf{x}, t) + \frac{1}{c} \mathbf{v} \times \mathbf{B}(\mathbf{x}, t) \right] \cdot \frac{\partial f}{\partial \mathbf{u}} = 0, \quad (49)$$

where

$$\frac{c}{\gamma} \mathbf{u} = \mathbf{v}$$

and

$$\gamma = (1 - v^2/c^2)^{-1/2} = (1 + u^2)^{1/2}$$

are the Minkowski velocity (\mathbf{u}) and relativistic mass ratio, respectively. The current density is now given by

$$\mathbf{J}(\mathbf{x}, t) = q \int \frac{c}{\gamma} \mathbf{u} f(\mathbf{x}, \mathbf{u}, t) d^3 u. \quad (50)$$

We linearize the above equation about the equilibrium state of an arbitrary velocity distribution, and assume the space and time dependence of the perturbed quantities as given in equation (1). The linearized perturbed current density for the beam becomes

$$\begin{aligned} \frac{4\pi i \omega}{c^2} \mathbf{J}_{1B} = & - \frac{4\pi q_B^2 n_B}{m_0 c^2} \int \frac{d^3 u f_0(\mathbf{u})}{\gamma \left(\omega - \frac{c}{\gamma} \mathbf{k} \cdot \mathbf{u} \right)^2} \\ & \times \left\{ \left(\omega - \frac{c}{\gamma} \mathbf{k} \cdot \mathbf{u} \right) \left[\omega \boldsymbol{\epsilon} - \frac{\omega(\mathbf{u} \cdot \boldsymbol{\epsilon})}{\gamma^2} \mathbf{u} + \frac{c}{\gamma} \mathbf{u} \times (\mathbf{k} \times \boldsymbol{\epsilon}) \right] \right. \\ & \left. + \frac{c}{\gamma} \mathbf{u} \mathbf{k} \cdot \left[\omega \boldsymbol{\epsilon} - \frac{\omega(\mathbf{u} \cdot \boldsymbol{\epsilon})}{\gamma^2} \mathbf{u} + \frac{c}{\gamma} \mathbf{u} \times (\mathbf{k} \times \boldsymbol{\epsilon}) \right] \right\}, \quad (51) \end{aligned}$$

where $f_0(\mathbf{u})$ is the normalized equilibrium distribution function of the beam particles, i.e.

$$\int d^3 u f_0(\mathbf{u}) = 1.$$

If the distribution function is a delta function in energy (velocity), i.e.

$$f_0(\mathbf{u}) = \delta(\mathbf{u} - \mathbf{u}_B),$$

then the perturbed current density becomes that given in equation (8) indicating that the results obtained in this section reduce to those of Section 2 in the limit of zero energy spread.

We further assume that there is energy spread of the beam particles in the direction of the beam only, which makes the equilibrium distribution function assume the form

$$f_0(\mathbf{u}) = \delta(u_x) \delta(u_z) f_{0y}(u_y). \quad (52)$$

Integrating over u_x and u_z and defining the following velocity integrals,

$$\begin{aligned}
 T_n &= \int_{-\infty}^{\infty} \frac{du_y f_{0y}(u_y) v_y^n}{\gamma_y (\omega - k_y v_y)}, \quad n = 0, 1, 2 \\
 U_n &= \int_{-\infty}^{\infty} \frac{du_y f_{0y}(u_y) v_y^{n+1}}{\gamma_y (\omega - k_y v_y)^2}, \quad n = 0, 1, 2
 \end{aligned}
 \tag{53}$$

the perturbed current density becomes

$$\begin{aligned}
 \frac{4\pi i \omega}{c^2} \mathbf{J}_{1B} &= -\frac{4\pi q_B^2 n_B}{m_0 c^2} \left\{ \omega T_0 \boldsymbol{\epsilon} - \omega \epsilon_y \frac{T_2}{c^2} \hat{\mathbf{y}} + T_1 \hat{\mathbf{y}} \times (\mathbf{k} \times \boldsymbol{\epsilon}) \right. \\
 &\quad \left. + \hat{\mathbf{y}} \left[\omega U_0 \mathbf{k} \cdot \boldsymbol{\epsilon} - \omega \epsilon_y k_y \frac{U_2}{c^2} + \mathbf{k} \cdot [\hat{\mathbf{y}} \times (\mathbf{k} \times \boldsymbol{\epsilon})] U_1 \right] \right\}, \tag{54}
 \end{aligned}$$

where

$$\int_{-\infty}^{\infty} du_y f_{0y}(u_y) = 1$$

and

$$\gamma_y = (1 + u_y^2)^{1/2} = (1 - v_y^2/c^2)^{-1/2}$$

$$v_y = \frac{cu_y}{\gamma_y}.$$

If we now combine the above result with equation (7), and insert into the wave equation, we obtain for the extraordinary mode the following dispersion equation in the limit of large $k_x c$:

$$\begin{aligned}
 (\omega_H^2 - \omega^2) + \frac{4\pi q_B^2 n_B}{m_0} \left\{ (\omega^2 - \omega_{CP}^2) \left(U_{-1} - \frac{U_1}{c^2} \right) + \omega_{PP}^2 \frac{U_1}{c^2} \right\} \\
 + \left(\frac{4\pi q_B^2 n_B}{m_0} \right)^2 (\omega^2 - \omega_{CP}^2) \left[\frac{U_{-1} U_1 - U_0^2}{c^2} \right] = 0. \tag{55}
 \end{aligned}$$

Square distribution

As an attempt to understand the effect of energy spread on the unstable mode, we consider a ‘‘square’’ distribution in beam particle velocities centered about the mono-energetic value, u_{yB} . That is, we let $f_{0y}(u_y)$ be of the form

$$\begin{aligned}
 f_{0y}(u_y) &= \frac{1}{\Delta}, \quad u_{yB} - \Delta/2 \leq u_y \leq u_{yB} + \Delta/2 \\
 &= 0 \quad \text{otherwise,}
 \end{aligned}
 \tag{56}$$

where the energy or velocity spread is represented by the parameter Δ . Inserting this distribution into the velocity integrals of equation (55), and assuming that the energy spread in the beam is small, i.e.

$$\Delta \ll u_{yB}, \tag{57}$$

we obtain after expanding the numerator and denominator of the integrand of the

velocity integrals in powers of the variable u , the following:

$$\begin{aligned}
 U_{-1} &= \frac{1}{\Delta\gamma_B(k_y V_B)^2} \int_{-\Delta/2}^{\Delta/2} du \frac{1 - \frac{V_B/c}{\gamma_B} u + \frac{2\gamma_B^2 - 3}{2\gamma_B^4} u^2 + \dots}{D} \\
 \frac{U_0}{c} &= \frac{V_B/c}{\Delta\gamma_B(k_y V_B)^2} \int_{-\Delta/2}^{\Delta/2} du \frac{1 - \frac{2V_B^2/c^2 - 1}{\gamma_B V_B/c} u + \frac{\gamma_B^2 - 4}{\gamma_B^4} u^2 + \dots}{D} \\
 \frac{U_1}{c^2} &= \frac{V_B^2/c^2}{\Delta\gamma_B(k_y V_B)^2} \int_{-\Delta/2}^{\Delta/2} du \frac{1 - \frac{3V_B^2/c^2 - 2}{\gamma_B V_B/c} u + \frac{2\gamma_B^4 - 15\gamma_B^2 + 15}{2\gamma_B^4(\gamma_B^2 - 1)} u^2 + \dots}{D},
 \end{aligned} \tag{58}$$

where

$$D = \left(\frac{\omega - k_y V_B}{k_y V_B} \right)^2 - \frac{2}{\gamma_B^3 V_B/c} \left(\frac{\omega - k_y V_B}{k_y V_B} \right) u + \left[\frac{1}{\gamma_B^2 - 1} + 3 \frac{\omega - k_y V_B}{k_y V_B} \right] \frac{u^2}{\gamma_B^4} + \dots$$

For a highly relativistic beam ($\gamma_B \gg 1$) we can approximate the integrals by keeping terms through u^2 in both the numerator and denominator. Such an approximation allows us to consider energy spreads which are larger or smaller than the resonant frequency term, $\omega - k_y V_B$.

“Small” beam energy spread

We assess the initial effects of energy spread by assuming that

$$\Delta \left(\frac{\beta_B}{\gamma_B^3} \right) \ll \left| \frac{\omega - k_y V_B}{k_y V_B} \right|, \tag{59}$$

which we call the “small” beam energy spread limit. In this limit, the dispersion equation becomes

$$\begin{aligned}
 & (\omega_H^2 - \omega^2) + \frac{\omega_{PB}^2 \omega^2 - \omega_H^2 + \gamma_B^2 \omega_{PP}^2}{\gamma_B^2} \frac{\omega^2 - \omega_{CP}^2}{(\omega - l\omega_{CB})^2} - \frac{\omega_{PB}^2}{\gamma_B^2} \frac{\Delta^2}{24\gamma_B^4} \frac{1}{(\omega - k_y V_B)^4} \\
 & \times \left\{ (\omega^2 - \omega_{CP}^2) \left[-3(4\gamma_B^2 - 5)(\omega - l\omega_{CB})^2 + 18l\omega_{CB}(\omega - l\omega_{CB}) - \frac{6l^2\omega_{CB}^2}{\gamma_B^2 - 1} \right] \right. \\
 & \left. - \omega_{PP}^2 [(2\gamma_B^4 - 15\gamma_B^2 + 15)(\omega - l\omega_{CB})^2 - 2(5\gamma_B^2 - 9)l\omega_{CB}(\omega - l\omega_{CB}) + 6l^2\omega_{CB}^2] \right\} \\
 & + 2 \frac{\omega_{PB}^4 (\omega^2 - \omega_{CP}^2)}{\gamma_B^2 (\omega - l\omega_{CB})^4} \frac{\Delta^2}{24\gamma_B^4} \cong 0. \tag{60}
 \end{aligned}$$

Solutions to this equation for plasma densities where normal mode-beam resonance occurs ($l = 10, 11, 12, \dots$), the addition of energy spread into the beam particles produces an initial increase in the growth rate of the cold beam-cold plasma unstable mode. For beam harmonics below the plasma electron frequency ($l < 9$), we find there exists a critical plasma density above which energy spread has a stabilizing effect

and below which it has the opposite effect. It appears then that at small energy spreads the expected stabilization does not occur for harmonics below and above the plasma electron cyclotron frequency at the appropriate plasma densities.

“Large” beam energy spread

We shall refer to the opposite limit of equation (59) as the “large” beam energy spread limit;

$$\Delta \left(\frac{\beta_B}{\gamma_B^3} \right) \gg \left| \frac{\omega - k_y V_B}{k_y V_B} \right|. \tag{61}$$

In this limit, the following dispersion relation is obtained:

$$\begin{aligned} (\omega_H^2 - \omega^2) - \frac{\omega_{PB}^2 (\omega^2 - \omega_H^2 + \gamma_B^2 \omega_{PP}^2)}{2\gamma_B^2 (\omega - l\omega_{CB})^2} \\ - \frac{3}{4} \frac{\omega_{PB}^4 (\omega^2 - \omega_{CP}^2)}{\gamma_B^4 l^2 \omega_{CB}^2 (\omega - l\omega_{CB})^2} \gamma_B^2 (\gamma_B^2 - 1) \cong 0, \end{aligned} \tag{62}$$

which represents the “zeroth” order dispersion relation in the “large” beam energy spread limit.

For beam harmonics below the plasma electron cyclotron frequency, $l < \gamma_B$, one can calculate from equation (62) a plasma density, $\omega_{PP} = \hat{\omega}_{PP}$, where the quantity $(\omega - l\omega_{CB})^2$ is zero. The result is

$$\left(\frac{\hat{\omega}_{PP}}{\omega_{CP}} \right)^2 = \frac{(\gamma_B^2 - l^2)}{\gamma_B^2 (\gamma_B^2 - 1)} \left\{ 1 + \frac{3}{2} \frac{\gamma_B^2 - 1}{l^2} \frac{\omega_{PB}^2}{\omega_{CB}^2} \right\}, \tag{63}$$

which yields:

$$(\omega - l\omega_{CB})^2 > 0, \text{ for } \omega_{PP} > \hat{\omega}_{PP}, \text{ implying stability} \tag{64}$$

and

$$(\omega - l\omega_{CB})^2 < 0, \text{ for } \omega_{PP} < \hat{\omega}_{PP}, \text{ implying instability.}$$

Table 7 lists values of $\hat{\omega}_{PP}$ for Astron parameters. Comparing the stability conditions for the “large” energy spread limit and for the case of a cold beam (Section 2), we find that the two conditions are almost reversed. For example, at the $l = 8$ beam harmonic the cold beam case indicates instability for plasma densities $\omega_{PP}/\omega_{CP} \geq 0.051$, whereas, for the present case, instability is indicated for $\omega_{PP}/\omega_{CP} \leq 0.055$.

TABLE 7. CRITICAL PLASMA DENSITY FOR “HIGH” TEMPERATURE BEAM FOR BEAM HARMONICS $l < \gamma_B = 9.0$

| l | $\hat{\omega}_{PP}/\omega_{CP}$ |
|-----|---------------------------------|
| 8 | 0.055 |
| 7 | 0.078 |
| 6 | 0.095 |
| 5 | 0.111 |
| 4 | 0.129 |
| 3 | 0.156 |
| 2 | 0.210 |
| 1 | 0.383 |

If one takes into account the experimental evidence that the beam-plasma interaction does not occur until sufficient plasma density is attained, corresponding to $\omega_{PB}/\omega_{CB} = 0.3$, the present results indicate that all beam harmonics less than the plasma electron cyclotron frequency are stable. We must keep in mind however that the dispersion equation is not valid at plasma densities far from $\omega_{PP} = \hat{\omega}_{PP}$, and thus this equation can only provide indications of the stabilizing effects due to energy spread in the limit of "large" energy spread.

For the beam harmonic which is coincident with the plasma electron cyclotron frequency, $l = \gamma_B = 9.0$, we find only stable modes, which again is a reversal from the cold beam case where instability existed at all plasma densities.

The remaining group of harmonics are those above the plasma electron cyclotron frequency, namely $l > \gamma_B$. Three regions of plasma density are examined separately. The first region is for densities below the hybrid density for a given beam harmonic. In this case, the dispersion relation gives:

$$(\omega - l\omega_{CB})^2 < 0, \quad \text{for } \omega_{PP} < \omega_{PP}^*, \quad \text{implying instability.} \quad (65)$$

For a plasma density greater than the hybrid density the result becomes

$$(\omega - l\omega_{CB})^2 > 0, \quad \text{for } \omega_{PP} > \omega_{PP}^*, \quad \text{implying stability.} \quad (66)$$

Since the analysis becomes more difficult in the vicinity of the hybrid density, only the solution at exactly the hybrid density is obtained. This solution is

$$\frac{\omega - l\omega_{CB}}{l\omega_{CB}} = \frac{1}{2} \left[\frac{\omega_{PB}^2 l^2 - \gamma_B^2}{\omega_{CB}^2 4l^4} \right]^{1/3} \{1 + i\sqrt{3}\}, \quad (67)$$

for $\omega_{PP} = \omega_{PP}^*$, which clearly does not satisfy the condition in equation (61). However, it may be indicative of the fact that probably an unstable mode exists at the hybrid density. We observe, nevertheless, the similarity between the growth rate in this "large" energy spread limit and the comparable cold temperature limit result of Section 2, i.e. equation (26). The difference between the two results, however, is that for the cold beam case the unstable mode appears below the beam harmonic, while in the present case it appears above the harmonic. Again, as for the other harmonics ($l < \gamma_B$ and $l = \gamma_B$) the two stability conditions are essentially reversed.

From the standpoint of Astron, where energy spread of the beam increases with time, we can visualize the beam-plasma interaction to initially occur with an essentially monoenergetic beam. As the energy spread in the beam increases, it ultimately becomes sufficient to quench the instability. For a rigorous theoretical verification of these postulated events, an analytical model which incorporates the mechanism of changing energy spread with time or with plasma density will be required. But, from the present preliminary calculations, we conjecture that it plays a major role in suppressing the instabilities in Astron. This role is seen mainly in the non-existence of unstable modes for harmonics $l < \gamma_B$, and the quenching of unstable modes for beam harmonics above the plasma electron cyclotron frequency, $l > \gamma_B$.

As in the section on collisional effects, we compare the present results with those obtained by other authors on the streaming instability. Again, we find that our results readily reduce to those of BÖHMER *et al.* (1971) and that of SINGHAUS (1964).

Specifically, we find that if we substitute the growth rate given by equation (22) into the non-relativistic limit of our definition as given in equation (61), we obtain

$$\frac{c\Delta}{V_B} \frac{\omega_{PP}}{\omega_{PB}} \gg 1,$$

which is essentially identical to the definition of "high" beam temperature used by Singhaus. These authors find in the "high" temperature limit that instabilities persist in a narrow region about the plasma frequency, which in their case ($\mathbf{B}_0 = 0$) is the normal mode corresponding to our hybrid frequency. Their conclusion agrees with ours in that sufficient energy spread may stabilize all beam harmonics except those in the immediate vicinity of the plasma normal modes.

6. CONCLUSIONS

We have put forth a model that describes the beam-plasma interaction and corresponding instabilities in Astron. This model shows that for a cold beam-cold plasma system the strongest interaction occurs at beam harmonics in the vicinity of the plasma upper hybrid frequency. When plasma thermal effects are included the model shows that interaction also occurs for beam harmonics above integral multiples of the plasma electron cyclotron frequency.

The introduction of collisions between the plasma electrons and the background neutral gas seems to indicate that collisional effects are most dominant in the immediate vicinity of the plasma normal modes. It is also shown that collision frequencies of the order of the beam cyclotron frequency can lead to stabilization of beam-plasma interactions in this vicinity.

The effects of energy spread in beam particles appear to be so profound that the instability conditions for a cold beam become totally reversed for "large" energy spreads. This reversal indicates possible stabilization of all harmonics below the electron cyclotron frequency, i.e. $l < \gamma_B$, and at sufficiently high plasma density for those harmonics in the region of the plasma normal modes.

These results are in good agreement with experimental observations and with results obtained in connection with a comparable phenomenon, namely, the streaming instability.

Acknowledgement—This work was initiated when one of us (C. D. S.) spent the summer of 1970 at Lawrence Livermore Laboratory working with Dr. MARVIN E. RENSINK in the Theoretical Group of the CTR Division. Dr. RENSINK's continued guidance throughout the work is greatly appreciated. Appreciation also goes to Dr. YOON II CHANG for his aid on computer programming.

REFERENCES

- BERNSTEIN I. B. (1958) *Phys. Rev.* **109**, 10.
 BOGDANKEVICH L. S. and RUKHADZE A. A. (1971) *Soviet Phys. Usp.* **14**, 163.
 BÖHMER H., CHANG J. and RAETHER M. (1971) *Phys. Fluids* **14**, 150.
 BRIGGS R. J. (1964) *Electron-Stream Interaction with Plasmas*. M.I.T. Press, Massachusetts.
 CHRISTOFILOS N. C. (1958) *Proc. Second U.N. Conf. Peaceful Uses Atomic Energy*, Vol. 32, p. 279.
 CHRISTOFILOS N. C. and FOWLER T. K. (1968) Rep. UCRL-50355.
 FESSENDEN T. J. and STALLARD B. W. (1970) CTR Annual Report, LRL, UCRL-50002-70, pg. 3-27.
 GRADSHTEYN I. S. and RYZHIK I. M. (1965) *Table of Integrals, Series and Products*. Academic Press, New York.
 HOLT E. H. and HASKELL R. E. (1965) *Foundations of Plasma Dynamics*. Macmillan, New York.
 KAINER S., DAWSON J. and SHANNY R. (1972) *Phys. Fluids* **15**, 493.
 KUSSE B. R. and BERS A. (1970) *Phys. Fluids* **13**, 2372.

- LOVELACE R. V. and SUDAN R. N. (1971) *Phys. Rev. Lett.* **27**, 1256.
 MONTGOMERY C. G. and TIDMAN D. A. (1964) *Plasma Kinetic Theory*. McGraw-Hill, New York.
 SELF S. A., SHOUCRI M. M. and CRAWFORD F. W. (1971) *J. appl. Phys.* **42**, 704.
 SINGHAUS H. E. (1964) *Phys. Fluids* **7**, 1534.
 STIX T. H. (1962) *The Theory of Plasma Waves*. McGraw-Hill, New York.
 STRIFFLER C. D. (1972) Ph.D. Thesis, Department of Nuclear Engineering, University of Michigan, Ann Arbor, Michigan.
 SUDAN R. N. (1965) *Phys. Fluids* **8**, 153.
 WATSON K. M., BLUDMAN S. A. and ROSENBLUTH M. N. (1960) *Phys. Fluids* **3**, 741 and 747.

APPENDIX

In this appendix we demonstrate the mathematical similarity of the dispersion relation obtained in Section 2 for large wave numbers and that obtained for electrostatic oscillations in a beam-plasma system. The latter results in the streaming instability as discussed by BRIGGS (1964).

The dispersion relation as given in equation (13) represents waves whose propagation and electric field vectors lie in a plane perpendicular to the applied magnetic field, \mathbf{B}_0 . If, in this equation, or better yet in equation (11), we let

$$\begin{aligned} k_x &= 0 \\ B_0 &= 0, \end{aligned} \tag{A1}$$

and consider the mode

$$\epsilon_x = \epsilon_z = 0, \quad \epsilon_y \neq 0, \tag{A2}$$

then for waves propagating along the beam, i.e. for

$$\mathbf{k} \parallel \mathbf{v}_B \parallel \boldsymbol{\epsilon}, \tag{A3}$$

the dispersion relation becomes

$$\omega^2 - \omega_{PB}^2 - \frac{\omega_{PB}^2}{\gamma_B^2} \frac{\omega^2}{(\omega - k_y V_B)^2} = 0. \tag{A4}$$

This equation represents a monoenergetic beam streaming through a cold background plasma, and its similarity to equation (19) is obvious. The important observation, here, is that the mechanisms that result in the unstable modes, and the stabilizing effects of collisions and energy spread in both our model and the streaming instability are similar (WATSON *et al.*, 1960; SINGHAUS, 1964; BÖHMER *et al.*, 1971; SELF *et al.*, 1971).